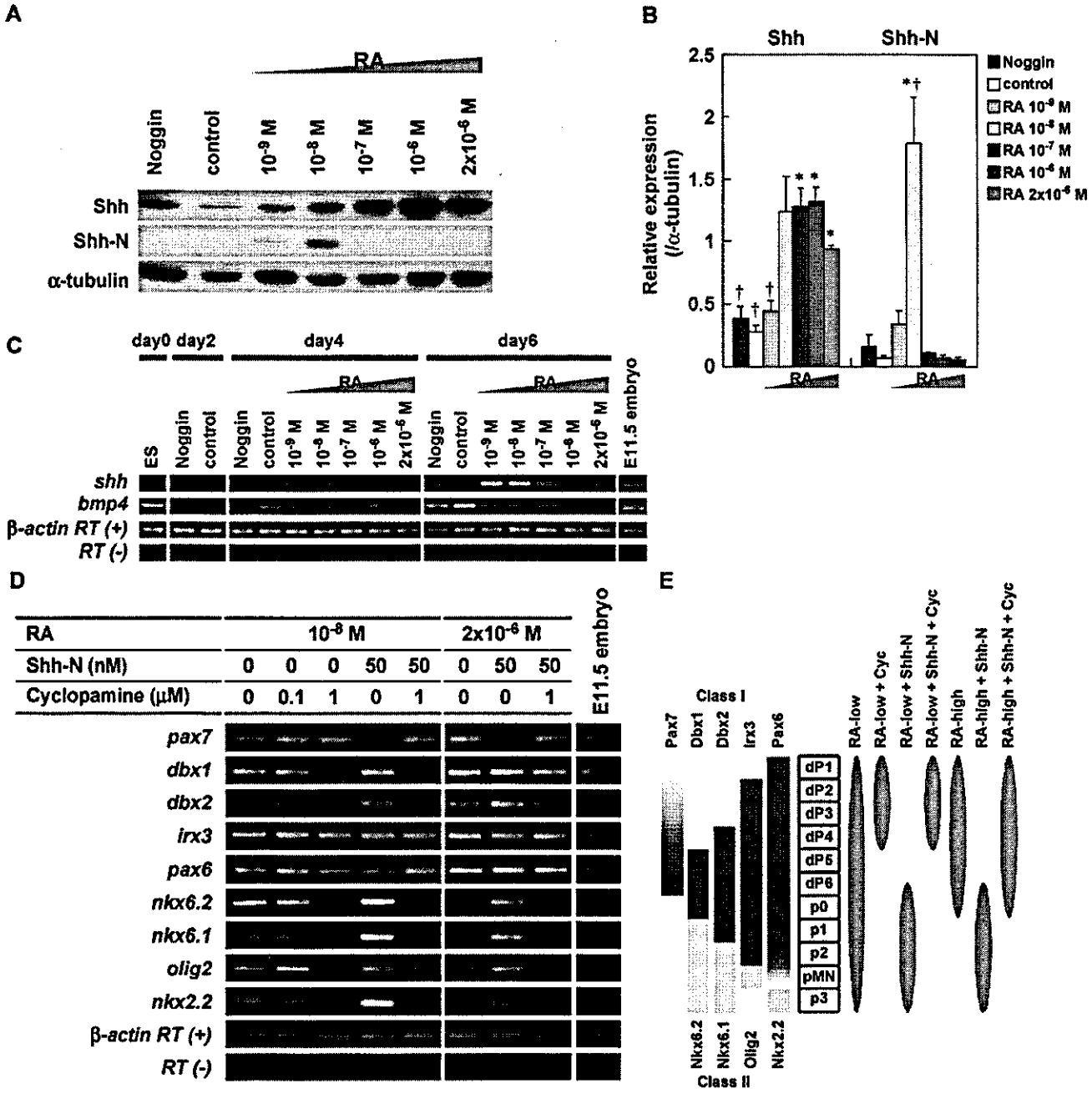

Fig. 7. Shh-N mediates RA-dependent dorso-ventral specification of ES-cell-derived neural progenitors. (A) Expression of Shh and its active N-terminal truncated form, Shh-N, in EBs cultured for 6 days, was analyzed by Western blotting. EBs were exposed to various concentrations of RA. Quantitative analysis was performed with Scion Image. The amounts of proteins were normalized to those of α-tubulin (B) ($n = 3$, mean ± SEM, *, $P < 0.05$ vs. control. †, $P < 0.05$ vs. RA 2×10^{-6} M). (C) RT-PCR analysis of *shh* and *bmp4*. Shh-N was more highly expressed in EBs treated with low-RA (10^{-9} M–10^{-8} M). (D) RT-PCR analysis of RA-exposed EBs treated with Shh-N and its inhibitor cyclopamine. Shh-N and cyclopamine were added together with RA on day 2. (E) Summary of expression patterns in vitro corresponding to in vivo. Cells from low-RA-treated EBs were a mixed population of dorsal-to-ventral neural progenitors and were capable of being dorsalized by inhibiting Shh signaling with cyclopamine. By contrast, exogenous Shh-N induced ventral neural progenitors were capable of being dorsalized by cyclopamine. Cells from high-RA-treated EBs showed dorsal positional identities. However, addition of Shh-N increased the number of ventral neural progenitors, and they were also capable of being dorsalized by cyclopamine treatment.

Fig 8. Dorso-ventral specification of RA treated EBs is altered by Shh-N and cyclopamine. The alteration of dorso-ventral identity by RA, Shh-N, and cyclopamine was confirmed by the immunostaining of dissociated EBs with antibodies against Pax7 as a marker for dorsal neural progenitors, against Nkx6.1 as a marker for ventral neural progenitors, and against Nkx2.2 as a marker for ventralmost neural progenitors in combination with Group B1 Sox or Nestin as a marker for neural progenitors. Immunoreactive cells as a percentage of the total number of cells counted on the basis of the nuclear staining with hoechst33342 are shown in B ($n = 3$, mean ± SEM). Scale bar: 50 μm.

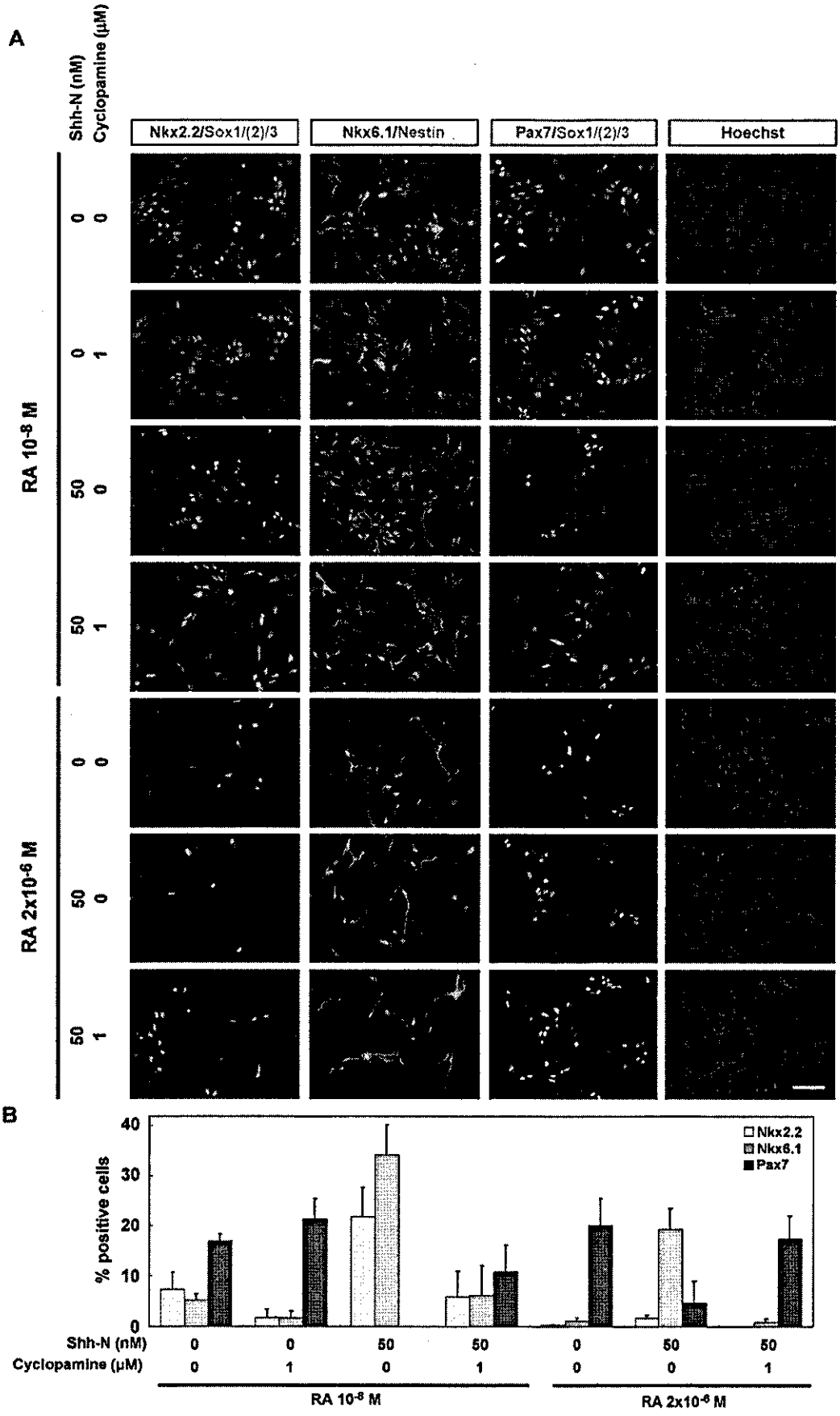
A
Shh-N (nM)
Cyclopamine (μM)
Nkx2.2/Sox1/(2)/3
Nkx6.1/Nestin
Pax7/Sox1/(2)/3
Hoechst
RA 10-8 M
RA 2x10-6 M
0 0
0 1
50 0
50 1
B
% positive cells
Nkx2.2
Nkx6.1
Pax7
Shh-N (nM) 0 0 50 50 0 50 50
Cyclopamine (μM) 0 1 0 1 0 0 1
RA 10-8 M
RA 2x10-6 M

number of Nkx6.1- or Nkx2.2-positive ventral neural progenitors in EBs treated with low-RA. The observation in EBs treated with high-RA is consistent with the previous report (Wichterle et al., 2002).

One of the major dorsalizing molecules in the CNS, *bmp4* (Caspary and Anderson, 2003; Jessell, 2000; Knecht and Bronner-Fraser, 2002), was not very strongly affected by RA, Shh-N, or cyclopamine, suggesting a lesser contribution of the BMP signal to this RA-mediated dorso-ventral specification (Fig. 7C, data not shown). These results indicate that differentiating EBs were ventralized by low-RA through induction of endogenous Shh-N protein, and that the effect was abrogated by cyclopamine and enhanced by the addition of exogenous Shh signal (Figs. 7D,E and 8).

Positional identity regulated by the RA concentration is mainly determined during the first 2 days of exposure to RA

According to the RT-PCR analysis of EBs cultured according to the 2−/4+ protocol, the expression patterns of most of the regionally specific markers were determined by day 4 and maintained unchanged thereafter. This observation raised two possibilities. One possibility is that the first 2 days of exposure to RA are critical to the determination of positional identity, and the second is that the effect of the RA concentration was altered during the later culture period by degradation of RA. To determine which of these possibilities was true, we performed a RT-PCR analysis of EBs cultured according to other protocols in which the times when RA is added or the duration of exposure to RA (2−/2+/2−, 2−/2+/2+, and 4−/4+ protocols) is different from the 2−/4+ protocol (Suppl. Fig. 1). Expression of *oct3/4* had been maintained before the addition of RA, but no expression of other markers except *otx2*, whose mRNA was expressed even in undifferentiated ES cells, had been detected in any of the culture protocols, including the 4−/4+ protocol. The expression patterns of most of regionally specific markers were determined by day 4 of the 2−/2+/2− and 2−/2+/2+ or by day 6 of the 4−/4+ protocol, and were virtually the same in all protocols as observed in the 2−/4+ protocol, and they were maintained thereafter as well (Suppl. Fig. 2). Overall, positional identity is determined during the first 2 days of exposure to RA and is maintained thereafter regardless of the presence or absence of RA in later culture periods.

Discussion

The pluripotent embryonic stem cell is a valuable in vitro model for studying the effects of various factors on cell lineage decisions in very early embryonic stages of mammalian development, and the effect of RA signaling on the differentiation of ES cells and neural induction, in particular, has been extensively studied. In addition to previous reports showing that RA promotes neural differentiation of ES cells and caudalization of the positional identity of their progeny (Bain et al., 1995, 1996; Fraichard et al., 1995; Gajovic et al., 1997; Renoncourt et al., 1998; Strubing et al., 1995; Wichterle et al., 2002), the results of the present study demonstrate the novel and precise actions of RA on neural differentiation and acquisition of positional identity by ES-cell-derived neural cells.

Effect of the concentration of RA on ES cell differentiation

It is well known that exposure of growing EBs to high-RA markedly increases the rate of neural differentiation, whereas low-RA induces more mesodermal cells (Rohwedel et al., 1999). Higher concentrations of RA also promote faster differentiation of ES cells, as indicated by the pattern of *oct3/4* expression, which was down-regulated more rapidly in EBs exposed to higher concentrations of RA, and down-regulated more at day 6 than at day 4 (Fig. 2). The result of this study showed that RA also concentration-dependently facilitates terminal differentiation of neural cells derived from ES cells. The expression levels of markers of differentiated neurons and glia, i.e., of βIII-tubulin and GFAP, respectively, was higher in EBs treated with higher concentrations of RA, whereas the expression levels of markers of undifferentiated neural cells, i.e., of Nestin, Group B1 Sox, Olig2, and *sox1* mRNA, was inversely correlated with the concentration of RA (Figs. 2 and 3). The findings are consistent with a high-RA enhancing differentiation of neural progenitor cells, as described previously (Bain et al., 1995, 1996; Fraichard et al., 1995; Gajovic et al., 1997; Renoncourt et al., 1998; Strubing et al., 1995; Wichterle et al., 2002).

Down-regulation of Wnt signaling has been shown to be one of the mechanisms involved in RA-induced neural differentiation of mouse ES cells (Aubert et al., 2002). Interestingly, β-catenin, which is a key molecule in Wnt signaling, has been shown to interact directly with retinoid receptor RAR, but not with RXR, in a retinoid-dependent manner, and as a result retinoids decrease β-catenin-Lef/Tcf-mediated transactivation in cultured cells in a dose-dependent manner (Easwaran et al., 1999). Wnt3a signaling through Lef/Tcf1 has also been implicated in suppression of neural differentiation and induction of mesodermal differentiation in the mouse embryo (Galceran et al., 1999; Yamaguchi et al., 1999; Yoshikawa et al., 1997). These findings raise the possibility that the one of the effects of RA in EBs is to inhibit the Wnt-β-catenin anti-neural pathway by up-regulation of Secreted frizzled-related protein 2 (Sfrp2) (Aubert et al., 2002) and/or sequestration of β-catenin in a concentration-dependent manner, thereby resulting in the promotion of neural differentiation, and inversely in the suppression of mesodermal differentiation.

FGFs are another molecules that may be involved in the neurogenesis related to RA signaling. RA has been shown to promote neuronal differentiation by repressing FGF signalings from the posterior neural plate. Caudal FGF signalings

have the opposite effects and repress Raldh2 (RA synthesis) in the presomatic mesoderm and generic neuronal differentiation in chick early neural tube (Diez del Corral et al., 2003; Novitch et al., 2003). These observations raise the possibility that RA inhibits the action of endogenously generated FGFs in a concentration-dependent manner during the culture of EBs. Further study of the associations between these signals is required to clarify the mechanism underlying the RA-promoted neural differentiation of ES cells.

Acquisition of rostro-caudal identity depends on the concentration of RA

A previous study on chick embryos showed that the default identity of early neural tissue is a rostral location and that neural cells can be caudalized by exogenous factors, such as the caudalizing activity of paraxial mesoderm, FGFs, and retinoid from the mesoderm, which induce midbrain, hindbrain, and spinal cord characters, when applied during the appropriate period of development (Muhr et al., 1999).

RA is one of the factors, that has been shown to be involved in hindbrain patterning and the caudalization of neural tissues in the early embryonic CNS in vivo (Maden, 2002). The distribution of endogenous RA has been examined in mouse and chick embryos, by various method, including HPLC (high-performance liquid chromatography) (Horton and Maden, 1995; Maden et al., 1998), the use of *LacZ* reporter cells (Maden et al., 1998; Wagner et al., 1992), and the use of RARβ_2-*LacZ* transgenic mice (Reynolds et al., 1991; Zimmer, 1992). This distribution of endogenous RA is correlated with the opposing action of the two main enzymes involved in RA-metabolism, RA-synthesizing enzyme, Raldh2, which is most strongly expressed in the paraxial mesoderm adjacent to the rostral spinal cord with the rostral boundary of the presumptive first somite (Berggren et al., 1999), and the catabolizing enzyme, Cyp26a1, which is expressed in anterior neuroepithelium. These spatially distributed enzymes create a rostro-caudal RA concentration gradient in vivo (Abu-Abed et al., 2001; Fujii et al., 1997; Maden et al., 1998; Sakai et al., 2001; Swindell et al., 1999), with the peak RA concentration occurring at the hindbrain/spinal cord boundary, with levels gradually decreasing anterior and posterior to it. Furthermore, it has been suggested that the patterning of the rhombomere is influenced over time by the constant supply of RA from the paraxial mesoderm, where the neuroepithelium grows and moves away form this source of RA. These findings imply that the more posterior rhombomeres that develop later than the more anterior rhombomeres may have been exposed to higher concentration of RA, leading to the expression of more posterior genes (such as posterior *hox* genes), which require a higher concentration of RA for activation in vivo (Maden, 2002). Our findings are consistent with the above-described putative regulatory mechanism of hindbrain/rostral spinal cord positional specification correlated with the RA concentration gradient in vivo in the following manner. The default positional identity of ES-cell-derived neural cells is specified as anteriormost forebrain, which was acquired in the control and Noggin-exposed EBs. EBs treated with low-RA were specified as midbrain to hindbrain, which is generated earlier and require lower concentrations of RA in vivo, whereas EBs treated with high-RA were specified as posterior hindbrain to rostral spinal cord, which is generated later and requires higher concentrations of RA in vivo. In addition, the fact that even the EBs treated with high-RA expressed genes specific to rostral (*hoxc4* to *hoxc6*), but not to caudal spinal cord (*hoxc8* to *hoxc10*) is consistent with the putative gradient of endogenous RA in vivo with a higher concentration in the rostral spinal cord, and the proposed role of RA in rostral spinal cord determination (Liu et al., 2001). Moreover, other factors may be involved in the activation of RA-responsive genes and the specification of positional identity, such as RA binding proteins, including cellular retinoic acid binding protein (CRABP) 1, which limits the access of RA to the nuclear retinoid receptors. The spatiotemporal pattern of expression of CRABP1 suggests that the fine regional control of availability of RA to the nuclear receptors may also play an important role in the organization of the central nervous system and the differentiation of its progenitors in vivo (Leonard et al., 1995; Maden, 2001; Maden et al., 1992; Ruberte et al., 1993). The role of these RA binding proteins in the regulation of in vitro differentiation of ES-cell-derived neural cells should be investigated further in the future.

RA also affects dorso-ventral positional identity

In contrast to the acquisition of rostro-caudal identity, dorso-ventral identity was analyzed in terms of expression of the transcriptional control of the homeodomain (HD) and basic helix-loop-helix (bHLH) proteins. Previous studies have emphasized the role of Shh signaling in establishing the pattern of expression of ventral spinal cord patterning genes (Jessell, 2000). RA has also been reported to contribute to the ventral patterning of the spinal cord; that is, to the induction of ventral interneurons (V0 and V1) by inducing class I genes, including Dbx1, Dbx2, Evx1, Evx2, and En (Pierani et al., 1999), and to the specification of limb level motor neuron subtypes by the expression of Raldh2 in LMC (Sockanathan and Jessell, 1998). Furthermore, recent studies have revealed involvement of RA from the paraxial mesoderm in the timing of neurogenesis and the patterning of the ventral spinal cord regulating the expression of class I and class II genes via inhibition of FGF signals and in combination with Shh signals (Diez del Corral et al., 2003; Novitch et al., 2003). However, the results of our study showed that the concentration of RA to which EBs were exposed was critical for acquisition of dorso-ventral identity by differentiating ES cells, and the concentration dependency showed a bell-

shaped pattern. This was shown by the pattern of the expression of class I and class II genes (Figs. 6A,B), which determines the dorso-ventral progenitor domains of developing hindbrain and spinal cord. EBs exposed to high-RA exhibit mainly dorsal phenotypes, whereas EBs exposed to low-RA exhibit more ventral phenotypes (Figs. 6–8). The expression pattern of *olig2*, higher at day 4 in EBs treated with high-RA and at day 6 in those treated with low-RA, seems to conflict with this finding; however, there are several possible explanations. One is that this alteration of the expression pattern of *olig2* mimics that in vivo according to the stage of development, with expression in most of the undifferentiated neural/glial progenitor cells in the ventral half of the spinal cord occurring around the period of neural tube closure and later being restricted to the motor neuron domain (pMN domain) of the ventral ventricular region, where the progenitors of motor neurons and oligodendrocytes arise sequentially (Lu et al., 2000; Takebayashi et al., 2000; Zhou et al., 2001). Thus, both the cells collected at day 4 from EBs exposed to high-RA and those collected at day 6 from EBs exposed to low-RA may consist of multipotent neural progenitors expressing Olig2. Furthermore, the role of RA in motor neuron development, such as its effect on the expression of bHLH and HD transcription factors, including Olig2, varies with the stage of development, according to a previous study that analyzed chick spinal cord development (Novitch et al., 2003). Similar alteration of the effects of RA may occur in our culture system and be another possible explanation for the sequential expression pattern of *olig2* in EBs exposed to high-RA.

The ventralization of EBs treated with low-RA can be explained by the finding that the active form of Shh-N, which is secreted by the notochord and floor plate of the developing CNS and ventralizes gene expression of neural progenitors in a concentration-dependent manner in vivo (Jessell, 2000), is more highly expressed on day 6 in EBs treated with low-RA (Figs. 7A–C). The hypothesis that the concentration-dependent activity of RA that defines dorso-ventral identity is mediated by Shh-N was confirmed by the result of treatment with the inhibitor of Shh signaling, cyclopamine (Figs. 7D,E and 8) (Chen et al., 2002a,b; Incardona et al., 1998). Cyclopamine abrogated the ventralization activity of low-RA treatment, and addition of exogenous Shh-N more efficiently ventralized differentiating EB-derived cells that had been exposed to both low-RA and high-RA, in a cyclopamine-sensitive manner. The expression level of *bmp4*, which dorsalizes neural progenitor cells (Caspary and Anderson, 2003; Jessell, 2000; Knecht and Bronner-Fraser, 2002), was not very strongly affected by Shh-N or cyclopamine in EBs exposed to either low-RA or high-RA (Fig 7C, data not shown), indicating that BMP signaling is not the major contributor to RA-mediated dorso-ventral specification. Taken together, these findings suggest that Shh-N expressed in EBs exposed to low-RA may be one of the major signals that ventralize neural progenitors and induce expression of class II genes in addition to class I genes, and that the lack of the shh signal in EBs exposed to high-RA may result in expression of only class I genes and a more dorsalized phenotype, which can be ventralized by exogenous Shh-N protein. The results of this study are consistent with a previous report that RA enhances expression of class I genes, but not of class II genes, in developing chick spinal cord (Diez del Corral et al., 2003; Novitch et al., 2003), and that exogenous Shh-N is required in addition to high-RA for efficient generation of motor neurons during EB formation in vitro (Renoncourt et al., 1998; Wichterle et al., 2002). Because EBs exposed to low-RA are mixed populations and contain many mesodermal cells (Fig. 2) (Rohwedel et al., 1999), they may secrete larger amounts of Shh-N than EBs treated with high-RA, which contain smaller proportions of mesodermal cells.

The discrepancy in response to RA between full-length Shh expression and Shh-N expressions detected by Western blotting (Figs. 7A,B) may be another important finding in this study. In contrast to the expression of full-length Shh being observed in EBs treated with RA at concentration 10^{-8} M and above, generation of Shh-N was detected only in EBs exposed to lower concentrations of RA (Figs. 7A,B), indicating the possible existence of RA-dependent machinery controlling Shh-N production by modulating an auto-processing mechanism by the C-terminus of Shh, which processes full-length Shh into the N-terminus active form, or by altering degradation activity of Shh-N.

Use of mutant ES cells for *indian hedgehog (ihh)* and *smoothened (smo)* has shown that hedgehog signaling is also required for neural differentiation of mouse ES cells by RA (Maye et al., 2004). In our study, however, expression of Group B1 Sox and *sox1* mRNA in EBs treated with low- or high-RA and their dissociates were not down-regulated by cyclopamine (Fig. 8, data not shown), indicating that neural differentiation was not inhibited under our culture conditions even in the presence of cyclopamine. There are two possible explanations for this discrepancy. In our experiments, cyclopamine was added on day 2 after the start of ES cells differentiation, whereas in the mutant ES cells in which hedgehog signaling was disrupted it was disrupted at the start of differentiation, raising the possibility that hedgehog signaling may be one of the factors that is required for the initial commitment of neuroectodermal differentiation. The other possibility is that the concentration of cyclopamine used in our study may not have been adequate to completely block hedgehog signaling, and the residual signaling activity may have been sufficient for the transition of ES-cell-derived ectoderm into neuroectoderm, but not for the ventralization of neural cells.

The mechanism underlying these roles of hedgehog signals in differentiation and specification of ES-cell-derived neural cells needs to be elucidated in the future.

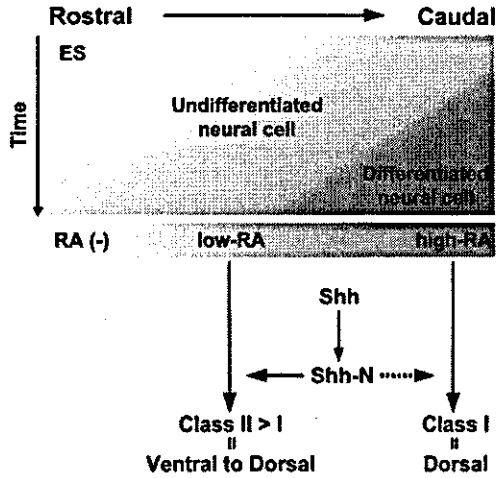

Fig 9. Schematic presentation of the concentration-dependent effects of RA on neural differentiation by mouse ES cells. RA simultaneously promotes both neural differentiation and caudalization in concentration-dependent manner. Low-RA induces a higher level of Shh-N, which endows ES-cell-derived neural progenitors with ventral identity, whereas high-RA poorly induces Shh-N, and they acquire dorsal neural identity instead.

RA is one of the most important inductive signals in vertebrate ontogeny and can be used to induce neural differentiation of mouse ES cells in vitro. However, its actions are complicated and difficult to deal with at will, because RA has the ability to induce various types of cells depending on its concentration, and it simultaneously affects both the timing of differentiation and the acquisition of positional identity, including rostro-caudal and dorso-ventral identity during neural differentiation (Fig. 9). Separation of these two phenomena is desirable to investigate the underlying mechanisms, and separation may have been accomplished, in part, by using SDIA, which is a culture protocol that induces neural cells without RA treatment. Thus, previous studies have shown involvement of RA at a single concentration in the caudalization of ES-cell-derived neural cells (Mizuseki et al., 2003; Wichterle et al., 2002). However, it is still not easy to separate these two phenomena completely during the neural induction of ES cells, because they are simultaneously affected by RA in vivo in combination with other signals, such as FGF and Shh signals, as shown by previous studies (Appel and Eisen, 2003; Diez del Corral et al., 2003; Novitch et al., 2003).

The present study identified detailed gene expression profiles and clarified the effects of the concentration of RA on ES cell differentiation, neuralization, and positional specification, though it may be impossible to map the patterns of expressions of the regional specific markers observed in ES-cell-derived neural cells directly to parallel expression of the markers in vivo. In combination with the RA-independent neural induction method using Noggin, this information will enable us to establish a strategy that will allow control of both the differentiation and the positional identity of neural cells derived from mouse ES cells through EB formation in vitro, and it may be applicable to human ES cells, raising the possibility of application to the treatment of neurological diseases.

Acknowledgments

We are grateful to Dr. H. Niwa for kindly providing ES cell line EB3, Dr. M. Nakafuku for the anti-Olig2 antibody, Dr. J.-F. Brunet for the anti-Phox2b antibody, Dr. O.D. Madsen and Dr. H. Duus for the anti-Nkx6.1 antibody, Dr. H. Kondoh for the anti-GroupB1 Sox antibody, Dr. Y. Takahashi for the xNoggin/BOS plasmid, J. Kohyama, S. Yuasa, and M. Yano for their thoughtful advice, and S. Nakamura for technical assistance. This work was supported by grants from CREST, Japan Society for the Promotion of Science to H.O.

Appendix A. Supplementary data

Supplementary data associated with this article can be found, in the online version, at doi:10.1016/j.ydbio.2004.07.038.

References

Abu-Abed, S., Dolle, P., Metzger, D., Beckett, B., Chambon, P., Petkovich, M., 2001. The retinoic acid-metabolizing enzyme, CYP26A1, is essential for normal hindbrain patterning, vertebral identity, and development of posterior structures. Genes Dev. 15, 226–240.

Acampora, D., Avantaggiato, V., Tuorto, F., Briata, P., Corte, G., Simeone, A., 1998. Visceral endoderm-restricted translation of Otx1 mediates recovery of Otx2 requirements for specification of anterior neural plate and normal gastrulation. Development 125, 5091–5104.

Appel, B., Eisen, J.S., 2003. Retinoids run rampant: multiple roles during spinal cord and motor neuron development. Neuron 40, 461–464.

Arber, S., Han, B., Mendelsohn, M., Smith, M., Jessell, T.M., Sockanathan, S., 1999. Requirement for the homeobox gene Hb9 in the consolidation of motor neuron identity. Neuron 23, 659–674.

Arceci, R., King, A., Simon, M., Orkin, S., Wilson, D., 1993. Mouse GATA-4: a retinoic acid-inducible GATA-binding transcription factor expressed in endodermally derived tissues and heart. Mol. Cell. Biol. 13, 2235–2246.

Aubert, J., Dunstan, H., Chambers, I., Smith, A., 2002. Functional gene screening in embryonic stem cells implicates Wnt antagonism in neural differentiation. Nat. Biotechnol. 20, 1240–1245.

Bain, G., Kitchens, D., Yao, M., Huettner, J.E., Gottlieb, D.I., 1995. Embryonic stem cells express neuronal properties in vitro. Dev. Biol. 168, 342–357.

Bain, G., Ray, W.J., Yao, M., Gottlieb, D.I., 1996. Retinoic acid promotes neural and represses mesodermal gene expression in mouse embryonic stem cells in culture. Biochem. Biophys. Res. Commun. 223, 691–694.

Berggren, K., McCaffery, P., Drager, U., Forehand, C.J., 1999. Differential distribution of retinoic acid synthesis in the chicken embryo as determined by immunolocalization of the retinoic acid synthetic enzyme, RALDH-2. Dev. Biol. 210, 288–304.

Blumberg, B., Bolado Jr., J., Moreno, T.A., Kintner, C., Evans, R.M.,

Papalopulu, N., 1997. An essential role for retinoid signaling in anteroposterior neural patterning. Development 124, 373–379.
Carpenter, E.M., 2002. Hox genes and spinal cord development. Dev. Neurosci. 24, 24–34.
Caspary, T., Anderson, K.V., 2003. Patterning cell types in the dorsal spinal cord: what the mouse mutants say. Nat. Rev., Neurosci. 4, 289–297.
Chen, J.K., Taipale, J., Cooper, M.K., Beachy, P.A., 2002a. Inhibition of Hedgehog signaling by direct binding of cyclopamine to Smoothened. Genes Dev. 16, 2743–2748.
Chen, J.K., Taipale, J., Young, K.E., Maiti, T., Beachy, P.A., 2002b. Small molecule modulation of Smoothened activity. Proc. Natl. Acad. Sci. 99, 14071–14076.
Diez del Corral, R., Olivera-Martinez, I., Goriely, A., Gale, E., Maden, M., Storey, K., 2003. Opposing FGF and retinoid pathways control ventral neural pattern, neuronal differentiation, and segmentation during body axis extension. Neuron 40, 65–79.
Easwaran, V., Pishvaian, M., Salimuddin, S., Byers, S., 1999. Cross-regulation of [beta]-catenin-LEF/TCF and retinoid signaling pathways. Curr. Biol. 9, 1415–1418.
Finley, M.F., Devata, S., Huettner, J.E., 1999. BMP-4 inhibits neural differentiation of murine embryonic stem cells. J. Neurobiol. 40, 271–287.
Fraichard, A., Chassande, O., Bilbaut, G., Dehay, C., Savatier, P., Samarut, J., 1995. in vitro differentiation of embryonic stem cells into glial cells and functional neurons. J. Cell Sci. 108 (Pt 10), 3181–3188.
Fujii, H., Sato, T., Kaneko, S., Gotoh, O., Fujii-Kuriyama, Y., Osawa, K., Kato, S., Hamada, H., 1997. Metabolic inactivation of retinoic acid by a novel P450 differentially expressed in developing mouse embryos. EMBO J. 16, 4163–4173.
Gajovic, S., St-Onge, L., Yokota, Y., Gruss, P., 1997. Retinoic acid mediates Pax6 expression during in vitro differentiation of embryonic stem cells. Differentiation 62, 187–192.
Galceran, J., Farinas, I., Depew, M.J., Clevers, H., Grosschedl, R., 1999. Wnt3a−/− like phenotype and limb deficiency in Lef1−/−Tcf1−/− mice. Genes Dev. 13, 709–717.
Gratsch, T.E., O'Shea, K.S., 2002. Noggin and chordin have distinct activities in promoting lineage commitment of mouse embryonic stem (ES) cells. Dev. Biol. 245, 83–94.
Helms, A.W., Johnson, J.E., 2003. Specification of dorsal spinal cord interneurons. Curr. Opin. Neurobiol. 13, 42–49.
Herrmann, B.G., Labeit, S., Poustka, A., King, T.R., Lehrach, H., 1990. Cloning of the T gene required in mesoderm formation in the mouse. Nature 343, 617–622.
Hitoshi, S., Tropepe, V., Ekker, M., van der Kooy, D., 2002. Neural stem cell lineages are regionally specified, but not committed, within distinct compartments of the developing brain. Development 129, 233–244.
Hooper, M., Hardy, K., Handyside, A., Hunter, S., Monk, M., 1987. HPRT-deficient (Lesch–Nyhan) mouse embryos derived from germline colonization by cultured cells. Nature 326, 292–295.
Horton, C., Maden, M., 1995. Endogenous distribution of retinoids during normal development and teratogenesis in the mouse embryo. Dev. Dyn. 202, 312–323.
Incardona, J., Gaffield, W., Kapur, R., Roelink, H., 1998. The teratogenic Veratrum alkaloid cyclopamine inhibits sonic hedgehog signal transduction. Development 125, 3553–3562.
Jensen, J., Serup, P., Karlsen, C., Nielsen, T.F., Madsen, O.D., 1996. mRNA profiling of rat islet tumors reveals Nkx 6.1as a beta -Cell-specific homeodomain transcription factor. J. Biol. Chem. 271, 18749–18758.
Jessell, T.M., 2000. Neuronal specification in the spinal cord: inductive signals and transcriptional codes. Nat. Rev., Genet. 1, 20–29.
Jonsson, J., Carlsson, L., Edlund, T., Edlund, H., 1994. Insulin-promoter-factor 1 is required for pancreas development in mice. Nature 371, 606–609.
Kawasaki, H., Mizuseki, K., Nishikawa, S., Kaneko, S., Kuwana, Y., Nakanishi, S., Nishikawa, S.I., Sasai, Y., 2000. Induction of midbrain dopaminergic neurons from ES cells by stromal cell-derived inducing activity. Neuron 28, 31–40.
Kawasaki, H., Suemori, H., Mizuseki, K., Watanabe, K., Urano, F., Ichinose, H., Haruta, M., Takahashi, M., Yoshikawa, K., Nishikawa, S., Nakatsuji, N., Sasai, Y., 2002. Generation of dopaminergic neurons and pigmented epithelia from primate ES cells by stromal cell-derived inducing activity. Proc. Natl. Acad. Sci. U. S. A. 99, 1580–1585.
Kessel, M., 1992. Respecification of vertebral identities by retinoic acid. Development 115, 487–501.
Kessel, M., Gruss, P., 1991. Homeotic transformations of murine vertebrae and concomitant alteration of Hox codes induced by retinoic acid. Cell 67, 89–104.
Kim, J.H., Auerbach, J.M., Rodriguez-Gomez, J.A., Velasco, I., Gavin, D., Lumelsky, N., Lee, S.H., Nguyen, J., Sanchez-Pernaute, R., Bankiewicz, K., McKay, R., 2002. Dopamine neurons derived from embryonic stem cells function in an animal model of Parkinson's disease. Nature 418, 50–56.
Knecht, A.K., Bronner-Fraser, M., 2002. Induction of the neural crest: a multigene process. Nat. Rev., Genet. 3, 453–461.
Kohtz, J.D., Lee, H.Y., Gaiano, N., Segal, J., Ng, E., Larson, T., Baker, D.P., Garber, E.A., Williams, K.P., Fishell, G., 2001. N-terminal fatty-acylation of sonic hedgehog enhances the induction of rodent ventral forebrain neurons. Development 128, 2351–2363.
Kohyama, J., Abe, H., Shimazaki, T., Koizumi, A., Okano, H., Hata, J., Umezawa, A., Nakashima, K., Taga, T., Gojo, S., 2001. Brain from bone: Efficient "meta-differentiation" of marrow stroma-derived mature osteoblasts to neurons with Noggin or a demethylating agent. Differentiation 68, 235–244.
Komuro, I., Izumo, S., 1993. Csx: a murine homeobox-containing gene specifically expressed in the developing heart. Proc. Natl. Acad. Sci. 90, 8145–8149.
Lee, S.H., Lumelsky, N., Studer, L., Auerbach, J.M., McKay, R.D., 2000. Efficient generation of midbrain and hindbrain neurons from mouse embryonic stem cells. Nat. Biotechnol. 18, 675–699.
Leonard, L., Horton, C., Maden, M., Pizzey, J.A., 1995. Anteriorization of CRABP-I expression by retinoic acid in the developing mouse central nervous system and its relationship to teratogenesis. Dev. Biol. 168, 514–528.
Lints, T., Parsons, L., Hartley, L., Lyons, I., Harvey, R., 1993. Nkx-2.5: a novel murine homeobox gene expressed in early heart progenitor cells and their myogenic descendants. Development 119, 419–431.
Liu, J.P., Laufer, E., Jessell, T.M., 2001. Assigning the positional identity of spinal motor neurons: rostrocaudal patterning of Hox-c expression by FGFs, Gdf11, and retinoids. Neuron 32, 997–1012.
Lu, Q.R., Yuk, D.-i., Alberta, J.A., Zhu, Z., Pawlitzky, I., Chan, J., McMahon, A.P., Stiles, C.D., Rowitch, D.H., 2000. Sonic hedgehog-regulated oligodendrocyte lineage genes encoding bHLH proteins in the mammalian central nervous system. Neuron 25, 317–329.
Maden, M., 2001. Role and distribution of retinoic acid during CNS development. Int. Rev. Cytol. 209, 1–77.
Maden, M., 2002. Retinoid signalling in the development of the central nervous system. Nat. Rev., Neurosci. 3, 843–853.
Maden, M., Horton, C., Graham, A., Leonard, L., Pizzey, J., Siegenthaler, G., Lumsden, A., Eriksson, U., 1992. Domains of cellular retinoic acid-binding protein I (CRABP I) expression in the hindbrain and neural crest of the mouse embryo. Mech. Dev. 37, 13–23.
Maden, M., Sonneveld, E., van der Saag, P., Gale, E., 1998. The distribution of endogenous retinoic acid in the chick embryo: implications for developmental mechanisms. Development 125, 4133–4144.
Marquardt, T., Pfaff, S.L., 2001. Cracking the transcriptional code for cell specification in the neural tube. Cell 106, 651–654.
Marshall, H., Nonchev, S., Sham, M.H., Muchamore, I., Lumsden, A., Krumlauf, R., 1992. Retinoic acid alters hindbrain Hox code and induces transformation of rhombomeres 2/3 into a 4/5 identity. Nature 360, 737–741.

Marti, E., Takada, R., Bumcrot, D., Sasaki, H., McMahon, A., 1995. Distribution of Sonic hedgehog peptides in the developing chick and mouse embryo. Development 121, 2537–2547.

Maye, P., Becker, S., Siemen, H., Thorne, J., Byrd, N., Carpentino, J., Grabel, L., 2004. Hedgehog signaling is required for the differentiation of ES cells into neurectoderm. Dev. Biol. 265, 276–290.

McGowan, K.M., Coulombe, P.A., 1998. Onset of keratin 17 expression coincides with the definition of major epithelial lineages during skin development. J. Cell Biol. 143, 469–486.

Mizuguchi, R., Sugimori, M., Takebayashi, H., Kosako, H., Nagao, M., Yoshida, S., Nabeshima, Y., Shimamura, K., Nakafuku, M., 2001. Combinatorial roles of olig2 and neurogenin2 in the coordinated induction of pan-neuronal and subtype-specific properties of motoneurons. Neuron 31, 757–771.

Mizuseki, K., Sakamoto, T., Watanabe, K., Muguruma, K., Ikeya, M., Nishiyama, A., Arakawa, A., Suemori, H., Nakatsuji, N., Kawasaki, H., Murakami, F., Sasai, Y., 2003. Generation of neural crest-derived peripheral neurons and floor plate cells from mouse and primate embryonic stem cells. Proc. Natl. Acad. Sci. U. S. A. 100, 5828–5833.

Muhr, J., Graziano, E., Wilson, S., Jessell, T.M., Edlund, T., 1999. Convergent inductive signals specify midbrain, hindbrain, and spinal cord identity in gastrula stage chick embryos. Neuron 23, 689–702.

Niederreither, K., Vermot, J., Schuhbaur, B., Chambon, P., Dolle, P., 2000. Retinoic acid synthesis and hindbrain patterning in the mouse embryo. Development 127, 75–85.

Niwa, H., Miyazaki, J., Smith, A.G., 2000. Quantitative expression of Oct-3/4 defines differentiation, dedifferentiation or self-renewal of ES cells. Nat. Genet. 24, 372–376.

Novitch, B.G., Chen, A.I., Jessell, T.M., 2001. Coordinate regulation of motor neuron subtype identity and pan-neuronal properties by the bHLH repressor Olig2. Neuron 31, 773–789.

Novitch, B.G., Wichterle, H., Jessell, T.M., Sockanathan, S., 2003. A requirement for retinoic acid-mediated transcriptional activation in ventral neural patterning and motor neuron specification. Neuron 40, 81–95.

Offield, M., Jetton, T., Labosky, P., Ray, M., Stein, R., Magnuson, M., Hogan, B., Wright, C., 1996. PDX-1 is required for pancreatic outgrowth and differentiation of the rostral duodenum. Development 122, 983–995.

Okabe, S., Forsberg-Nilsson, K., Spiro, A.C., Segal, M., McKay, R.D., 1996. Development of neuronal precursor cells and functional postmitotic neurons from embryonic stem cells in vitro. Mech. Dev. 59, 89–102.

Pattyn, A., Morin, X., Cremer, H., Goridis, C., Brunet, J., 1997. Expression and interactions of the two closely related homeobox genes Phox2a and Phox2b during neurogenesis. Development 124, 4065–4075.

Pattyn, A., Hirsch, M., Goridis, C., Brunet, J., 2000. Control of hindbrain motor neuron differentiation by the homeobox gene Phox2b. Development 127, 1349–1358.

Pevny, L.H., Sockanathan, S., Placzek, M., Lovell-Badge, R., 1998. A role for SOX1 in neural determination. Development 125, 1967–1978.

Pierani, A., Brenner-Morton, S., Chiang, C., Jessell, T.M., 1999. A sonic hedgehog-independent, retinoid-activated pathway of neurogenesis in the ventral spinal cord. Cell 97, 903–915.

Porter, J.A., von Kessler, D.P., Ekker, S.C., Young, K.E., Lee, J.J., Moses, K., Beachy, P.A., 1995. The product of hedgehog autoproteolytic cleavage active in local and long-range signalling. Nature 374, 363–366.

Porter, J.A., Ekker, S.C., Park, W.J., von Kessler, D.P., Young, K.E., Chen, C.H., Ma, Y., Woods, A.S., Cotter, R.J., Koonin, E.V., Beachy, P.A., 1996. Hedgehog patterning activity: role of a lipophilic modification mediated by the carboxy-terminal autoprocessing domain. Cell 86, 21–34.

Renoncourt, Y., Carroll, P., Filippi, P., Arce, V., Alonso, S., 1998. Neurons derived in vitro from ES cells express homeoproteins characteristic of motoneurons and interneurons. Mech. Dev. 79, 185–197.

Reynolds, K., Mezey, E., Zimmer, A., 1991. Activity of the beta-retinoic acid receptor promoter in transgenic mice. Mech. Dev. 36, 15–29.

Roelink, H., Porter, J.A., Chiang, C., Tanabe, Y., Chang, D.T., Beachy, P.A., Jessell, T.M., 1995. Floor plate and motor neuron induction by different concentrations of the amino-terminal cleavage product of sonic hedgehog autoproteolysis. Cell 81, 445–455.

Rohwedel, J., Guan, K., Wobus, A.M., 1999. Induction of cellular differentiation by retinoic acid in vitro. Cells Tissues Organs 165, 190–202.

Ross, S.A., McCaffery, P.J., Drager, U.C., De Luca, L.M., 2000. Retinoids in Embryonal Development. Physiol. Rev. 80, 1021–1054.

Ross, S.E., Greenberg, M.E., Stiles, C.D., 2003. Basic helix-loop-helix factors in cortical development. Neuron 39, 13–25.

Ruberte, E., Friederich, V., Chambon, P., Morriss-Kay, G., 1993. Retinoic acid receptors and cellular retinoid binding proteins: III. Their differential transcript distribution during mouse nervous system development. Development 118, 267–282.

Sakai, Y., Meno, C., Fujii, H., Nishino, J., Shiratori, H., Saijoh, Y., Rossant, J., Hamada, H., 2001. The retinoic acid-inactivating enzyme CYP26 is essential for establishing an uneven distribution of retinoic acid along the anterio-posterior axis within the mouse embryo. Genes Dev. 15, 213–225.

Schuurmans, C., Guillemot, F., 2002. Molecular mechanisms underlying cell fate specification in the developing telencephalon. Curr. Opin. Neurobiol. 12, 26–34.

Shimazaki, T., Shingo, T., Weiss, S., 2001. The ciliary neurotrophic factor/leukemia inhibitory factor/gp130 receptor complex operates in the maintenance of mammalian forebrain neural stem cells. J. Neurosci. 21, 7642–7653.

Sive, H.L., Draper, B.W., Harland, R.M., Weintraub, H., 1990. Identification of a retinoic acid-sensitive period during primary axis formation in *Xenopus laevis*. Genes Dev. 4, 932–942.

Smith, W.C., Harland, R.M., 1992. Expression cloning of noggin, a new dorsalizing factor localized to the Spemann organizer in *Xenopus* embryos. Cell 70, 829–840.

Sockanathan, S., Jessell, T.M., 1998. Motor neuron-derived retinoid signaling specifies the subtype identity of spinal motor neurons. Cell 94, 503–514.

Strubing, C., Ahnert-Hilger, G., Shan, J., Wiedenmann, B., Hescheler, J., Wobus, A.M., 1995. Differentiation of pluripotent embryonic stem cells into the neuronal lineage in vitro gives rise to mature inhibitory and excitatory neurons. Mech. Dev. 53, 275–287.

Swindell, E.C., Thaller, C., Sockanathan, S., Petkovich, M., Jessell, T.M., Eichele, G., 1999. Complementary domains of retinoic acid production and degradation in the early chick embryo. Dev. Biol. 216, 282–296.

Takebayashi, H., Yoshida, S., Sugimori, M., Kosako, H., Kominami, R., Nakafuku, M., Nabeshima, Y., 2000. Dynamic expression of basic helix-loop-helix Olig family members: implication of Olig2 in neuron and oligodendrocyte differentiation and identification of a new member, Olig3. Mech. Dev. 99, 143–148.

Temple, S., 2001. The development of neural stem cells. Nature 414, 112–117.

Tonegawa, A., Takahashi, Y., 1998. Somitogenesis controlled by noggin. Dev. Biol. 202, 172–182.

Tropepe, V., Hitoshi, S., Sirard, C., Mak, T.W., Rossant, J., van der Kooy, D., 2001. Direct neural fate specification from embryonic stem cells: a primitive mammalian neural stem cell stage acquired through a default mechanism. Neuron 30, 65–78.

Wagner, M., Han, B., Jessell, T., 1992. Regional differences in retinoid release from embryonic neural tissue detected by an in vitro reporter assay. Development 116, 55–66.

Wang, H.-F., Liu, F.-C., 2001. Developmental restriction of the LIM homeodomain transcription factor Islet-1 expression to cholinergic neurons in the rat striatum. Neuroscience 103, 999–1016.

Wichterle, H., Lieberam, I., Porter, J.A., Jessell, T.M., 2002. Directed differentiation of embryonic stem cells into motor neurons. Cell 110, 385–397.

Wilkinson, D.G., Bhatt, S., Herrmann, B.G., 1990. Expression pattern of the mouse T gene and its role in mesoderm formation. Nature 343, 657–659.

Wood, H.B., Episkopou, V., 1999. Comparative expression of the mouse Sox1, Sox2 and Sox3 genes from pre-gastrulation to early somite stages. Mech. Dev. 86, 197–201.

Wurst, W., Bally-Cuif, L., 2001. Neural plate patterning: upstream and downstream of the isthmic organizer. Nat. Rev. Neurosci. 2, 99–108.

Yamaguchi, T.P., Takada, S., Yoshikawa, Y., Wu, N., McMahon, A.P., 1999. T (Brachyury) is a direct target of Wnt3a during paraxial mesoderm specification. Genes Dev. 13, 3185–3190.

Ying, Q.L., Stavridis, M., Griffiths, D., Li, M., Smith, A., 2003. Conversion of embryonic stem cells into neuroectodermal precursors in adherent monoculture. Nat. Biotechnol. 21, 183–186.

Yoshikawa, Y., Fujimori, T., McMahon, A.P., Takada, S., 1997. Evidence that absence ofWnt-3aSignaling promotes neuralization instead of paraxial mesoderm development in the mouse. Dev. Biol. 183, 234–242.

Zhou, Q., Choi, G., Anderson, D.J., 2001. The bHLH transcription factor Olig2 promotes oligodendrocyte differentiation in collaboration with Nkx2.2. Neuron 31, 791–807.

Zimmer, A., 1992. Induction of a RAR beta 2-lacZ transgene by retinoic acid reflects the neuromeric organization of the central nervous system. Development 116, 977–983.

Zimmerman, L.B., De Jesus-Escobar, J.M., Harland, R.M., 1996. The Spemann organizer signal noggin binds and inactivates bone morphogenetic protein 4. Cell 86, 599–606.

ELSEVIER

Neuroscience Letters 363 (2004) 33–37

Neuroscience Letters

www.elsevier.com/locate/neulet

Isolation and transplantation of dopaminergic neurons generated from mouse embryonic stem cells

Takahito Yoshizaki[a,b,c], Motoki Inaji[d,g], Hiroko Kouike[a,c], Takuya Shimazaki[a,c], Kazunobu Sawamoto[a,c], Kiyoshi Ando[d,e], Isao Date[h], Kazuto Kobayashi[f], Tetsuya Suhara[d], Yasuo Uchiyama[b], Hideyuki Okano[a,c,*]

[a] *Department of Physiology, Keio University School of Medicine, Tokyo 160-8582, Japan*
[b] *Department of Cell Biology and Neuroscience, Osaka University Graduate School of Medicine, Osaka 565-0852, Japan*
[c] *Japan Science and Technology Agency, Core Research for Evolutional Science and Technology, Tokyo, Japan*
[d] *National Institute of Radiological Sciences, Chiba 263-8555, Japan*
[e] *Central Institute for Experimental Animals, Kanagawa 216-0001, Japan*
[f] *Department of Molecular Genetics, Institute of Biomedical Sciences, Fukushima Medical University School of Medicine, Fukushima 960-1295, Japan*
[g] *Department of Neurosurgery, Tokyo Medical and Dental University, Tokyo 113-8519, Japan*
[h] *Department of Neurological Surgery, Okayama University Graduate School of Medicine and Dentistry, Okayama 700-8530, Japan*

Received 16 January 2004; received in revised form 11 March 2004; accepted 12 March 2004

Abstract

Embryonic stem (ES) cells differentiate into dopamine (DA)-producing neurons when co-cultured with PA6 stromal cells, but the resulting cultures contain a variety of unidentified cells. In order to label live DA neurons in mixed populations, we introduced a GFP reporter under the control of the tyrosine hydroxylase (TH) gene promoter into ES cells. GFP expression was observed in TH-immunoreactive cells that differentiated from the ES cells that carried the *TH-GFP*reporter gene. DA neurons expressing GFP were sorted from the mixed cell population by fluorescence-activated cell sorting of cells exhibiting GFP fluorescence, and the sorted GFP^+ cells obtained were transplanted into a rat model of Parkinson's disease. Some of these cells survived and innervated the host striatum, resulting in a partial recovery from parkinsonian behavioral defects. This strategy of isolation and transplantation of ES-cell-derived DA neurons should be useful for cellular and molecular studies of DA neurons and for clinical application in the treatment of Parkinson's disease.

Keywords: Embryonic stem cells; Dopamine neuron; Transplantation; Stromal-cell derived inducing activity (SDIA); *TH-GFP*

Most of the symptoms of Parkinson's disease are caused by degeneration of dopamine (DA)-producing neurons in the substantia nigra [13], and intrastriatal grafting of DA neurons or their precursors has been reported to ameliorate the motor symptoms of patients with Parkinson's disease [10,16,20]. Although transplantation is considered a promising means of therapy, its clinical use is still restricted to only a few cases. The major factors limiting this therapy are the difficulty of obtaining sufficient donor cells and the controversial ethical and legal issues raised by the use of human fetal allografts [2,5], and as a result, a variety of strategies to generate DA neurons in vitro have been proposed to overcome these problems [3,4]. Techniques that convert neural progenitor cells into DA neurons after expansion of the population in vitro have been reported [8, 17], and protocols to induce DA neuronal differentiation from embryonic stem (ES) cells have also been reported [6, 7,9]. Because neural stem cells and ES cells can be easily expanded in vitro, these approaches seem capable of solving the problems mentioned above. ES cells, in particular, can be expected to provide an unlimited supply of donor source because of their unlimited capacity for self-renewal, but since after their induction the DA neurons generated in vitro exist within a mixed population, which may contain a variety of unidentified cells that might be tumorigenic and harmful to patients, they should be isolated before transplantation. We previously developed a technique for labeling DA neurons with GFP driven by the tyrosine

* Corresponding author. at Department of Physiology, Keio University School of Medicine, 35 Shinanomachi, Shinjuku-ku, Tokyo 160-8582, Japan. Tel.: +81-3-5363-3747; fax: +81-3-3357-5445.
E-mail address: hidokano@sc.itc.keio.ac.jp (H. Okano).

0304-3940/03/$ - see front matter © 2004 Elsevier Ireland Ltd. All rights reserved.
doi:10.1016/j.neulet.2004.03.074

hydroxylase (TH) gene promoter and then isolating the cells by fluorescence-activated cell sorting (FACS) [18], and in the present study, we applied it to isolation of ES-cell-derived DA neurons.

The *EB3* ES cells [15] were co-transfected with the p*TH-GFP* plasmid [18] and pMC1-neo plasmid (Stratagene) containing antibiotic resistant gene to obtain the stable transformant line *TH13D2*. They were maintained as described previously [6] in medium containing Geneticin. For differentiation, 5×10^5 *TH13D2* cells were dissociated to prepare a single-cell suspension and plated on confluent PA6 cells growing in a T-25 flask to induce neural differentiation as described previously [6]. To determine the dopamine levels in the conditioned medium, 1.3×10^5 ES cells were differentiated as above in 24-well plates for 12 days and incubated at 37 °C for 15 min in 500 μl of Hanks' balanced salt solution (HBSS) with 56 mM KCl. The conditioned medium was stabilized with 0.4 M perchloric acid and 5 mM EDTA and maintained at −80 °C until used for reverse-phase-HPLC analysis. FACS sorting of GFP^+ cells and transplantation into a rat model of Parkinson's disease were performed essentially as described previously [18]. All experimental protocols applied to animals were approved by the Animal Ethics Committee of Keio University. Female Sprague–Dawley rats (8 weeks old, weighing 180–220 g) were supplied by CLEA, Japan. Administration of 6-hydroxydopamine (6-OHDA) (2 μg/ml, Sigma) and rotational behavior due to the unilateral lesion were assessed essentially as described previously [19]. 6-OHDA was injected at the speed of 1 μl/min in the right substantia nigra (4 μl, AP −4.8 mm, ML +1.8 mm, DV −7.5 mm from bregma) and the right median forebrain bundle (4 μl, AP −4.5 mm, ML +1.6 mm, DV −7.8 mm from bregma) of adult female rats. Four weeks later, the efficacy of lesioning was assessed in all rats by testing them for ipsilateral rotational behavior and recording it on a video tape for 90 min after injection of methamphetamine (2.5 mg/kg, i.p.). The rats rotated more than 500/h were used for transplantation. FACS-sorted cells (1×10^4 cells/2 μl of differentiation medium [6], $n = 8$) or vehicle medium (2 μl, $n = 8$) were placed at the two sites in the striatum ipsilateral to the lesion (AP +1.0 mm, ML +3.0 mm, DV −5.0 mm; AP ± 0 mm, ML +3.0 mm, DV −5.0 mm) at the speed of 1 μl/min. There was no significant difference in rotation scores between the two groups (910 ± 127.6 vs. 813 ± 41.4, $P > 0.05$) before transplantation. All transplant recipients and vehicle control group were given cyclosporine A (10 mg/kg p.o., Novartis Pharma) daily. After another 4 weeks, the efficacy of transplantation was assessed in all rats by testing them for rotational behavior and recording it on a video tape after injection of methamphetamine (2.5 mg/kg, i.p.). Brain sections (50 μm) were cut on a Leica Vibratome VT1000 S (Leica Instruments) and after incubating with rabbit polyclonal anti-TH antibody (Chemicon AB152) for 48 h, with biotin-conjugated goat anti-rabbit IgG overnight, and then incubated with an ABC kit (Vector). For immunofluorescence staining, sections were incubated with rabbit polyclonal anti-TH antibody and monoclonal anti-GFP antibody (Molecular Probes A-11120) for 48 h, and then incubated with Alexa™ 488 goat anti-rabbit IgG antibody and Alexa™ 568 goat anti-mouse IgG antibody (Jackson Immuno Research) overnight for signal detection. Finally, the sections were stained with Hoechst 33342 (2 μg/ml, Sigma) to label all the nuclei. Immunohistochemical images were examined with a Zeiss-AxioCam microscope system.

To monitor induction of DA neurons by green fluorescence in vitro, we differentiated *TH13D2* cells into DA neurons by co-culture with the PA6 cells that possesses stromal-cell derived inducing activity (SDIA) [6]. Undifferentiated *TH13D2* cells do not express either TH or GFP (data not shown). During co-culture, GFP expression was detected in 36 ± 3.8% of the cells in the dishes at 4 days in vitro (DIV) ($n = 5$) and the percentage of GFP^+ cells gradually increased to 44 ± 4.1% by 12 DIV ($n = 5$) (Fig. 1A). TH expression was detected as early as 4 DIV in 3% of cells. The percentage of TH-immunoreactive cells increased to 32 ± 4.3% by 12 DIV ($n = 5$). At the end of co-culture, the cultures contained process-bearing putative DA neurons that expressed both GFP and TH, and round cells that expressed GFP but not TH (Fig. 1B). While the percentage of GFP^+ cells keep constant during co-culture, TH^+ cells increase rapidly, suggesting that the GFP^+ TH^- cells may represent precursors of TH^+ DA neurons. Consistently, the similar GFP^+ TH^- putative precursors have been found in the ventricular zone adjacent to DA neurons in the ventral mesencephalon of *TH-GFP*transgenic mouse embryos [11]. The 9-kb promoter of the rat TH gene we used in this study seems to possess *cis*-regulatory elements for transcriptional control that are sufficient for initial activation of the gene but not for the later phases. Consequently, expression of GFP in the *TH-GFP* transgenic mouse embryos started in developing midbrain DA neurons around E11–E12 and was then remarkably down-regulated during later embryonic stages [11]. Consistent with this, some of the TH-positive cells displaying the morphology of mature neurons did not express detectable GFP under our culture conditions (Fig. 1B). To confirm that these TH-positive cells were mature DA neurons, we determined secreted dopamine levels in the culture supernatant by HPLC (Fig. 1E). The total amount of dopamine production was 678 ± 79.8 pg/well per hour, and no dopamine-β-hydroxylase was detected by immunocytochemistry (data not shown). These results suggest that live DA neurons and their precursors generated from ES cells can be labeled with the *TH-GFP*reporter gene.

We previously established a method of isolating DA neurons from brain tissue of transgenic mice by FACS labeled with TH-GFP [18], and in this study we applied the same strategy to differentiated ES cells. *TH13D2* ES cells at 12 DIV after neural induction by the SDIA method were enzymatically dissociated and then analyzed for GFP fluorescence by flow cytometry (Fig. 2A,B). Dead cells

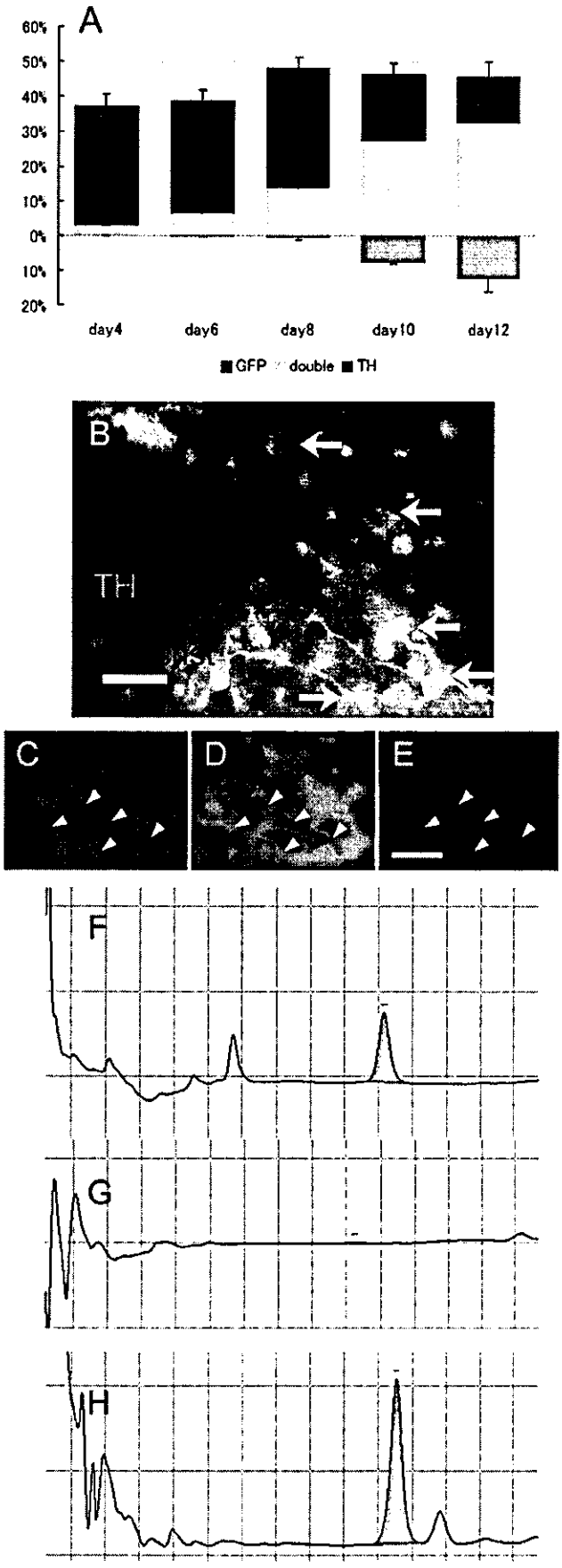

were excluded by gating on forward and side scatter as well as by elimination of propidium-iodide (PI)-positive events. To obtain a very pure population of GFP^+ DA neurons, cells were considered positive only if their fluorescence was brighter than that of the control cells. According to this criterion, only 2.66 ± 0.87% of the live cells were isolated as GFP^+ cells ($n = 5$); 89.2 ± 3.7% of GFP^+ cells were identified in the PI-positive cell population and 84.1 ± 5.3% of GFP^- cells were identified alive ($n = 5$). These results suggest that GFP^+ cells are preferentially killed, probably because they are process-bearing neurons and can be damaged by enzymatic and physical dissociation. The sorted GFP^+ cells were examined under a fluorescence microscope. Virtually all of the cells showed GFP fluorescence (Fig. 2C), confirming that a pure population of GFP^+ cells had been obtained. The cells were then fixed and stained for TH, and 98.2 ± 2.1% of the sorted GFP^+ cells were TH^+ ($n = 5$) (Fig. 2E). By contrast, only 2.8 ± 0.79% of all sorted whole live cells were GFP^+ ($n = 5$) (Fig. 2D), and 2.7 ± 1.05% were TH/GFP double-positive ($n = 5$). Thus, sorting based on TH-GFP fluorescence yielded a highly enriched population of DA neurons.

To investigate the function of the sorted GFP^+ cells in vivo, we transplanted them into the brain of a rat model of Parkinson's disease [1]. All of the animals with unilateral 6-OHDA lesions displayed a robust rotation response to methamphetamine before transplantation without a significant difference between the transplantation group and the vehicle control group ($P > 0.05$ unpaired two-tailed Student's t-test). A total of 20,000 sorted GFP^+ cells were transplanted in the lesioned striatum of each rat in the transplantation group. Four weeks after transplantation, a significant reduction in rotational asymmetry was observed in all of the rats transplanted with GFP^+ cells, but no significant improvement was detected in the lesion control animals (pre-transplant 813 ± 41.4 vs. post-transplant 914 ± 242.2, $P > 0.05$, $n = 8$). The rotation scores of the grafted animals ($n = 8$) were reduced by an average of 15.6 ± 7.3% ($P < 0.05$) compared with the pre-transplantation scores, indicating that the grafted cells were functional in vivo.

Fig. 1. Differentiation of TH-GFP transgenic ES cells in vitro. Changes in ratio of GFP-positive (green) and TH-positive (red) cells during differentiation. TH and GFP double positive cells (yellow) increased during induction. Cells in culture (day 12) were stained with antibodies against TH (red), GFP (green), and Hoechst 33342 (blue). The photograph is a merged image of anti-GFP-stained (green), anti-TH-stained (red), and Hoechst 33342-stained (blue) cells. Some cells have neuronal appearance (arrow). Scale bar = 160 μm. (C–E) High power magnification images of the cells of neuronal morphology indicated by arrow in (B) labeled with anti-GFP antibody (C), anti-TH antibody (D) and Hoechst (E). Axon-like process is marked by arrowheads. Scale bar = 160 μm. (F,G) HPLC detection of dopamine secreted in the DA standard with medium (F), medium control (G), and conditioned medium of DA neurons stimulated with KCl (H).

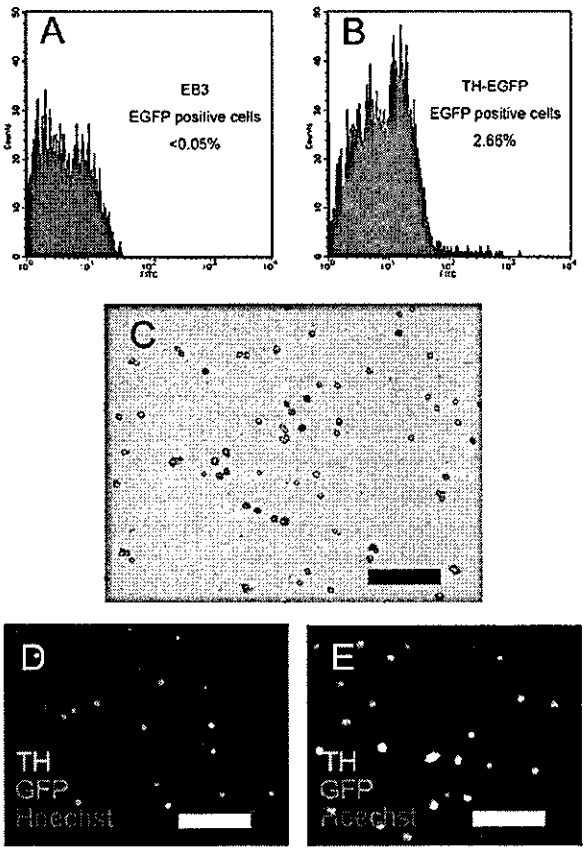

Fig. 2. Isolation of GFP-positive cells by FACS. After induction (12 DIV) cells from the control ES cell culture (A) and TH13D2 cell culture (B) were analyzed with a FACS. Virtually all the sorted cells show GFP fluorescence (C). Scale bar = 200 μm. Unsorted (D) and sorted GFP$^+$ (E) cells were directly attached to slides and fixed and stained with an antibody against TH (red), and GFP (green), and Hoechst 33342 (blue). The photographs are merged images of anti-GFP-stained (green), anti-TH-stained (red), and Hoechst 33342-stained (blue) cells. Scale bar = 200 μm.

Brain sections were stained with anti-TH antibody and anti-GFP antibody to identify grafted cells (Fig. 3B,C). The 6-OHDA lesions caused a virtually complete loss of TH$^+$ DA neurons in the substantia nigra and concomitant depletion of TH-immunoreactive fibers in the lesioned striatum (data not shown). Grafts that contained GFP$^+$ and TH$^+$ double-positive cells were found in the striatum of the rats transplanted with the GFP$^+$ cells (Fig. 3B,C), and some of the TH$^+$ cells in the grafts displayed morphological features suggestive of mature neurons and had extended TH$^+$ fibers into the host striatum (Fig. 3D). Taken together, these results show that the isolated GFP$^+$ cells differentiated into mature DA neurons in the host striatum and were functional and improved amphetamine-induced rotational asymmetry in a rat model of Parkinson's disease. ES-cell derived sorted GFP-positive cells, however, were less effective (77.3% vs. 15.6%) in achieving rotational recovery than transplantation of sorted GFP-positive cells from the ventral mesencephalon of TH-GFP transgenic mouse in our previous study [18]. Thus, the protocol for preparation of DA neurons from ES cells needs to be modified to increase

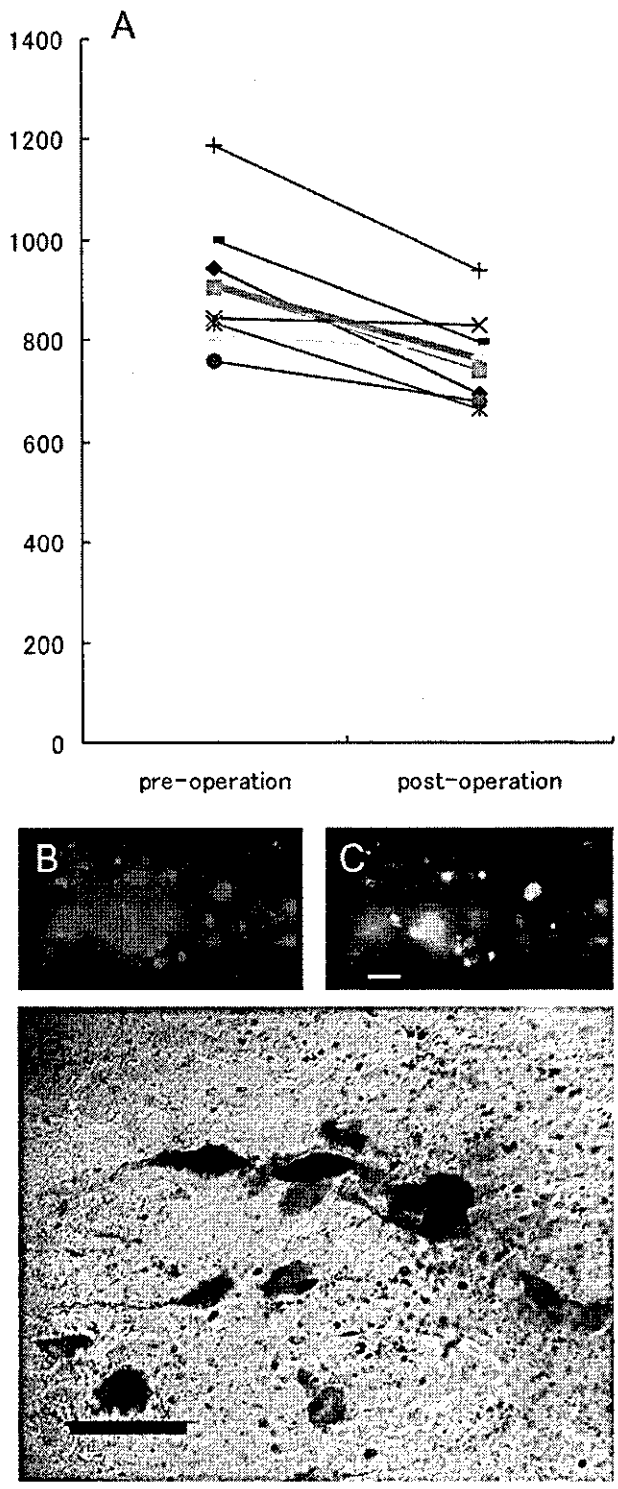

Fig. 3. Transplanted EGFP$^+$ cells caused functional recovery in a rat model of Parkinson's disease. (A) Net ipsilateral amphetamine-induced rotation asymmetry over the 90-min test session. All of the animals with grafts showed steady improvement compared with pre-graft rotation. Average rotations are represented by the thick red line. (B,C) The transplantation site. Grafted cells expressing both GFP (B) and TH (C) can be seen in the striatum. Scale bar = 80 μm. (D) High power magnification view of TH$^+$ neurons in the graft. The grafted TH-positive cells display the morphology of mature DA neurons. Scale bar = 80 μm.

the efficiency of recovery. Modification for obtaining higher amount of mature neurons in vitro such as administration of growth factors would be needed, or preparation conditions that mimic the differentiation of ventral mesencephalon. The number of surviving cells was much lower when dissociated cells were transplanted than when colonies were transplanted, indicating that colonies are more efficient for implanting TH-positive cells in vivo than cell suspension conditions [12]. Administration of neurotrophic factors should improve the survival of transplanted DA neurons [14].

To compare the tumorigenicity of the donor cells, we co-cultured the *CAG-GFP* ES cells that express GFP constitutively and *TH13D2* cells with PA6 cells for only 4 days, and transplanted sorted GFP^+ cells into the striatum. Four weeks later, we found tumor formation only in the brains that received the CAG-GFP-sorted mixed cell population (data not shown). These results suggest that transplantation of unsorted ES-derived cells may cause formation of a tumor in the brain, which may be prevented by use of FACS-isolated DA neurons.

In conclusion, we have demonstrated that ES-cell-derived functional DA neurons can be labeled with the TH-GFP reporter gene and isolated by FACS. This novel system should be useful for cellular and molecular studies of DA neurons and for clinical applications in the treatment of Parkinson's disease, and, in particular, it may significantly reduce the risk of tumor formation by ES-derived neural cells after transplantation.

Acknowledgements

We thank T. Nakano for the PA6 cells, H. Niwa for the EB3 ES cells and H.J. Okano for valuable discussion. This work was supported by a grant from the Ministry of Education, Science, Sports, Culture and Technology, a grant from CREST of the Japan Science and Technology Agency, and a grant-in-aid from the 21st Century COE Program of the Ministry of Education, Science and Culture to Keio University.

References

[1] M.F. Beal, Experimental models of Parkinson's disease, Nat. Review Neurosci. 2 (2001) 325–332.
[2] A. Björklund, S.B. Dunnett, P. Brundin, A.J. Stoessl, C.R. Freed, R.E. Breeze, M. Levivier, M. Peschanski, L. Studer, R. Barker, Neural transplantation for the treatment of Parkinson's disease, Lancet Neurol. 2 (2003) 437–445.
[3] L.M. Bjorklund, O. Isacson, Regulation of dopamine cell type and transmitter function in fetal and stem cell transplantation for Parkinson's disease, Prog. Brain Res. 138 (2002) 411–420.
[4] O. Isacson, L.M. Bjorklund, J.M. Schumacher, Toward full restoration of synaptic and terminal function of the dopaminergic system in Parkinson's disease by stem cells, Ann. Neurol. 53 (2003) S135–S148.
[5] O. Isacson, L. Costantini, J.M. Schumacher, F. Cicchetti, S. Chung, K.S. Kim, Cell implantation therapies for Parkinson's disease using neural stem, transgenic or xenogeneic donor cells, Parkinson Relat. Disord. 7 (2001) 205–212.
[6] H. Kawasaki, K. Mizuseki, S. Nishikawa, S. Kaneko, Y. Kuwana,, S. Nakanishi, S.I. Nishikawa, Y. Sasai, Induction of midbrain dopaminergic neurons from ES cells by stromal cell-derived inducing activity, Neuron 28 (2000) 31–40.
[7] J.H. Kim, J.M. Auerbach, J.A. Rodriguez-Gomez, I. Velasco, D. Gavin, N. Lumelsky, S.H. Lee, J. Nguyen, R. Sanchez-Pernaute, K. Bankiewicz, R. McKay, Dopamine neurons derived from embryonic stem cells function in an animal model of Parkinson's disease, Nature 418 (2002) 50–56.
[8] J.Y. Kim, H.C. Koh, J.Y. Lee, M.Y. Chang, Y.C. Kim, H.Y. Chung, H. Son, Y.S. Lee, L. Studer, R. McKay, S.H. Lee,, Dopaminergic neuronal differentiation from rat embryonic neural precursors by Nurr1 overexpression, J. Neurochem. 85 (2003) 1443–1454.
[9] S.H. Lee, N. Lumelsky, L. Studer, J.M. Auerbach, D. McKay, Efficient generation of midbrain and hindbrain neurons from mouse embryonic stem cells, Nat. Biotech. 18 (2000) 675–679.
[10] O. Lindvall, P. Brundin, H. Widner, S. Rehncrona, B. Gustavii, R. Frackowiak, L.S. Leenders, G. Sawle, J.C. Rothwell, C.D. Marsden, A. Bjorklund, Grafts of fetal dopamine neurons survive and improve motor function in Parkinson's disease, Science 247 (1990) 574–577.
[11] N. Matsushita, H. Okada, Y. Yasoshima, K. Takahashi, K. Kiuchi, K. Kobayashi, Dynamics of tyrosine hydroxylase promoter activity during midbrain dopaminergic neuron development, J. Neurochem. 82 (2002) 295–304.
[12] A. Morizane, J. Takahashi, Y. Takagi, Y. Sasai, N. Hashimoto, Optimal conditions for in vivo induction of dopaminergic neurons from embryonic stem cells through stromal cell-derived inducing activity, J. Neurosci. Res. 69 (2002) 934–939.
[13] T. Nagatsu, T. Yamaguchi, M.K. Rahman, J. Trocewicz, K. Oka, Y. Hirata, I. Nagatsu, H. Narabayashi, T. Kondo, R. Iizuka, Catecholamine-related enzymes and biopterin cofactor in Parkinson's diseases, in: R.G. Hasseler, J.F. Christ (Eds.), Advances in Neurology, 40, Raven, New York, 1984, pp. 467–473.
[14] K. Nakajima, H. Hida, Y. Shimano, I. Fujimoto, T. Hashitani, M. Kumazaki, T. Sakurai, H. Nishino, GDNF is a major component of trophic activity in DA-depleted striatum for survival and neurite extension of DAergic neurons, Brain Res. 916 (2001) 76–84.
[15] H. Niwa, J. Miyazaki, A.G. Smith, Quantitative expression of Oct-3/4 defines differentiation, dedifferentiation or self-renewal of ES cells, Nat. Genet. 24 (2000) 372–376.
[16] P. Piccini, D.J. Brooks, A. Björklund, R.N. Gunn, P.M. Grasby, O. Rimoldi, P. Brundin, P. Hagell, S. Rehncrona, H. Widner, O. Lindvall, Dopamine release from nigral transplants visualized in vivo in a Parkinson's patient, Nat. Neurosci. 2 (1999) 1137–1140.
[17] S.S. Riaz, E. Jauniaux, G.M. Stern, H.F. Bradford, The controlled conversion of human neural progenitor cells derived from foetal ventral mesencephalon into dopaminergic neurons in vitro, Dev. Brain Res. 136 (2002) 27–34.
[18] K. Sawamoto, N. Nakao, K. Kobayashi, N. Matsushita, H. Takahashi, K. Kakishita, A. Yamamoto, T. Yoshizaki, T. Terashima, F. Murakami, T. Itakura, H. Okano, Visualization, direct isolation, and transplantation of midbrain dopaminergic neurons, Proc. Natl. Acad. Sci. USA 98 (2001) 6423–6428.
[19] U. Ungerstedt, W. Arbuthnott, Quantitative recording of rotational behavior in rats after 6-hydroxy-dopamine lesions of the nigrostriatal dopamine system, Brain Res. 24 (1970) 485–493.
[20] G.K. Wenning, P. Odin, P. Morrish, S. Rehncrona, H. Widner, P. Brundin, J.C. Rothwell, R. Brown, B. Gustavii, P. Hagell, M. Jahanshahi, G. Sawle, A. Bjorklund, D.J. Brooks, C.D. Marsden, N.P. Quinn, O. Lindvall, Short- and long-term survival and function of unilateral intrastriatal dopaminergic grafts in Parkinson's disease, Ann. Neurol. 42 (1997) 95–107.

Nonrenewal of Neurons in the Cerebral Neocortex of Adult Macaque Monkeys

Daisuke Koketsu,[1] Akichika Mikami,[2] Yusei Miyamoto,[1] and Tatsuhiro Hisatsune[1]

[1]Department of Integrated Biosciences, University of Tokyo, Kashiwa 277-8562, Japan, and [2]Primate Research Institute, Kyoto University, Inuyama 484-8506, Japan

The concept that, after developmental periods, neocortical neurons become numerically stable and are normally nonrenewable has been challenged by a report of continuous neurogenesis in the association areas of the cerebral cortex in the adult Macaque monkey. Therefore, we have reexamined this issue in two different Macaque species using the thymidine analog bromodeoxyuridine (BrdU) as an indicator of DNA replication during cell division. We found several BrdU+/NeuN+ (neuronal nuclei) double-labeled cells, but cortical neurons, distinguished readily by their size and cytological and immunohistochemical properties, were not BrdU positive. We examined in detail the frontal cortex, where it is claimed that the largest daily addition of neurons has been made, but did not see migratory streams or any sign of addition of new neurons. Thus, we concluded that, in the normal condition, cortical neurons of adult primates, similar to other mammalian species, are neither supplemented nor renewable.

Key words: adult neurogenesis; cerebral cortex; primates; DNA synthesis; glial markers; 3D immunohistochemistry

Most neurons of the mammalian brain are generated from neuroepithelial cells near cerebral ventricles during well defined developmental stages and then act as substrates of neural circuitry throughout life (Rakic, 1985). However, recent findings of adult neurogenesis in selected structures of the mammalian brain present the possibility that this concept does not apply for all brain regions, in particular, the neural circuits of the olfactory bulb and dentate gyrus of the hippocampus, which may be changing their basic circuitry with the arrival of newly born neurons (Rochefort et al., 2002; van Praag et al., 2002). In addition, the application of new staining methods in the adult Macaque monkeys uncovered some new neurons in the olfactory bulb (Kornack and Rakic, 2001b) and dentate gyrus of the hippocampus (Gould et al., 1999a; Kornack and Rakic, 1999).

In terms of the cerebral neocortex, studies in various mammalian species that range from mice and rats to ferrets and cats have indicated that neurogenesis in this structure stops after well defined developmental periods (Hicks and D'Amato, 1968; Caviness and Sidman, 1973; Luskin and Shatz, 1985; Jackson et al., 1989; Takahashi et al., 1996). Furthermore, no sign of neuronal renewal has been found in the cortex of adult rodents (Magavi et al., 2000). An extensive analysis of Macaque monkeys exposed to [^{3}H]thymidine indicated that the neocortical neurons in primates are generated prenatally (Rakic, 1974) and not normally renewed during adulthood (Rakic, 1985, 2002a). It was suggested that a stable population of neurons in the cortex might be an important mechanism for continuity of learning and preserving memory over a lifetime (Rakic, 1985). Contrary to this theory, Gould and colleagues assert, on the basis of labeling with the thymidine analog bromodeoxyuridine (BrdU), that streams of new neurons are generated continuously and added to the association neocortex of adult Macaque monkeys (Gould et al., 1999b), where many form connections and survive for weeks before dying (Gould et al., 2001). The daily addition of thousands of new neurons to the principal sulcus alone (Gould et al., 1999b) in the absence of net growth indicated high turnover. To verify this claim, Kornack and Rakic (2001a) have performed experiments using the BrdU method in adult Macaque monkeys. They found BrdU-labeled non-neuronal cells, but they did not detect newly born neurons in the neocortex, nor did they find the stream of migrating neurons from the proliferative subventricular zone to the principal sulcus of the prefrontal cortex (Kornack and Rakic, 2001a). This discrepancy in basic findings required a reexamination in other laboratories (Nowakowski and Hayes, 2000).

Therefore, we addressed the question of whether new neurons are generated and continuously added in the neocortex of juvenile and young adult Macaque monkeys using BrdU methods for labeling DNA synthesis in the dividing brain cells (Nowakowski et al., 1989) that were used by previous investigators. We examined in detail the frontal cortex, where it has been previously claimed that the largest daily addition of neurons is made (Gould et al., 1999b). We selected juvenile and young adult monkeys because they presumably have more neuronal plasticity and to avoid the possibility of BrdU labeling during unscheduled DNA synthesis in the process of cell death (apoptosis) in aged animals (Yang et al., 2001). We also avoided high doses of BrdU to avoid its possible mutagenic and stimulation effect on DNA synthesis (Nowakowski and Hayes, 2001; Rakic, 2002b). To identify the phenotypes of BrdU-labeled cells in the neocortex, an immunohistochemical analysis was performed with neuronal markers NeuN, a transcriptional factor that is expressed in the nucleus and cytoplasm of neurons (Mullen et al., 1992), and doublecortin

Received Sept. 13, 2002; revised Nov. 4, 2002; accepted Nov. 20, 2002.

This study is supported by a Grant-in-Aid for Scientific Research from the Ministry of Education, Science, Sports and Culture of Japan. We thank Dr. Jose Antonio Campos-Ortega and Dr. Yukio Hirata for informative discussion and technical advice. We also thank Dr. Shinichi Kohsaka for kindly providing an anti-Iba-1 antibody.

Correspondence should be addressed to Tatsuhiro Hisatsune, Department of Integrated Biosciences, Graduate School of Frontier Sciences, The University of Tokyo, Bioscience Building 402, 5-1-5 Kashiwanoha, Kashiwa, Chiba 277-8562, Japan. E-mail: hisatsune@k.u-tokyo.ac.jp.

 0270-6474/03/230937-06$15.00/0

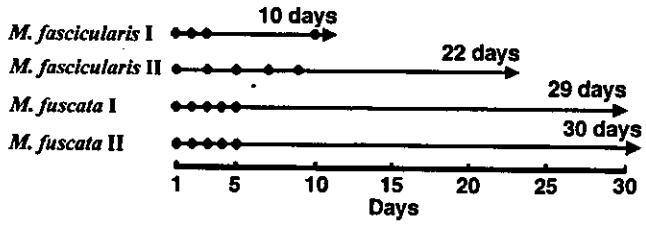

Figure 1. BrdU injection schedule. The day of BrdU injection is represented by the *filled circle*, and the day of perfusion is represented by the *arrowhead*. *M. fascicularis* I received once-daily BrdU injections for 3 consecutive days and one more injection after 7 d and then was perfused 1 d after the final injection. *M. fascicularis* II received five once-daily injections every other day and then was perfused 14 d after the final injection. *M. fuscata* I and *M. fuscata* II received once-daily injections for 5 consecutive days. Then, *M. fuscata* I and *M. fuscata* II were perfused 25 or 26 d after the final injection, respectively. The *number* of days represents the period between the first injection and perfusion.

(DCX) (Gleeson et al., 1999; Nacher et al., 2001) and also with markers of other non-neuronal cell types. GFAP and S-100β (astroglial cell), O4 (oligodendrocyte), and Iba-1 (microglial cell) (Ito et al., 1998) were used.

Materials and Methods

Animals. Two young adult female *Macaca fascicularis* (Cynomolgus monkey; 5 years of age) and two juvenile female *M. fuscata* (Japanese monkey; 2 years of age) were used. Monkeys were housed at the Primate Research Institute of Kyoto University and were maintained in individual cages with up to 16 cages facing each other in a single room. Thus, the monkeys could see and interact with other monkeys. In addition, Japanese monkeys were provided with a piece of wood that was hung in the cage as a playing tool and a food pickup toy that was placed in front of the cage every day for several hours. The size of the toy was 60 × 60 cm with 480 holes, half of which were covered with a piece of plate so that the monkey needed to use its fingers to carefully pick up the food (Saguinus, Monmouth, IL). The food used was raisins, and the monkeys usually picked up most of the raisins within several hours. The monkeys were cared for according to the *Guide for the Care and Use of Laboratory Animals* from the National Institutes of Health and the *Guide for Care and Use of Laboratory Primates* published by the Primate Research Institute, Kyoto University.

Injections of BrdU. Monkeys were injected with BrdU (Wako, Osaka, Japan) dissolved in 0.9% NaCl with 0.007 M NaOH. Two *M. fascicularis* were injected intravenously, whereas the *M. fuscata* received intraperitoneal injections. The first *M. fascicularis* (*M. fascicularis* I) received once-daily BrdU injections for 3 consecutive days and one more injection after another 7 d with a dose of 100 mg/kg body weight per injection; it was perfused 10 d after the initial BrdU injection, i.e., 1 day after the final BrdU injection (Fig. 1). The second *M. fascicularis* (*M. fascicularis* II) received five once-daily BrdU injections every other day with a dose of 75 mg/kg per injection; then, it was perfused 22 d after the initial BrdU injection, i.e., 14 d after the final BrdU injection. The first *M. fuscata* (*M. fuscata* I) received once-daily BrdU injections for 5 consecutive days with a dose of 75 mg/kg per injection; it was perfused 29 d after the initial BrdU injection, i.e., 25 d after the final BrdU injection. The second *M. fuscata* (*M. fuscata* II) received the same series of BrdU injections as *M. fuscata* I, but it was perfused 30 d after the initial BrdU injection, i.e., 26 d after the final BrdU injection. All animals were killed by intracardiac perfusion with 4% paraformaldehyde. All removed brains were postfixed with fresh 4% paraformaldehyde for 2 d at 4°C. This combination of injections and perfusion schedule allowed the exposure of newly generated cells as well as the ability to follow their migration and differentiation to the cortex as done on the hippocampus (Markakis and Gage, 1999).

Preparation of tissue sections. Postfixed brains were dissected into right and left hemispheres. Each hemisphere was cut into blocks of 5 mm. The brain blocks were put into O.C.T. Compound (Sakura, Tokyo, Japan), and frozen at −80°C. The frozen blocks were sliced into 40 μm coronal sections with a cryostat (MICROM, Walldorf, Germany). The sliced sections were preserved in a cryoprotectant solution (30% ethylene glycol, 30% glycerol in 0.05 M phosphate buffer) at −20°C until they were processed.

Immunohistochemistry. Sections were washed twice with Tris-buffered saline (TBS) for 10 min. Sections were then treated in 10 M citric acid buffer at 90°C for 5 min. The heated sections were left at room temperature for 30 min and washed with TBS for 10 min. The sections were incubated in 1 M HCl at 37°C for 30 min and neutralized by rinsing with 0.1 M borate buffer and washed twice with TBS. The sections were then blocked with a blocking solution (5% normal donkey serum and 0.3% Triton X-100 in TBS) for 30 min at room temperature with gentle shaking. The blocked sections were reacted with primary antibodies at 4°C. The concentration of Triton X-100 in the blocking solution dissolving primary antibodies with 1 or 3 d reaction time was 0.3 or 0.1%, respectively. Monoclonal rat anti-BrdU antibody (Harlan, Leicestershine, UK) with a 1:200 dilution and monoclonal mouse anti-BrdU (Becton Dickinson, Franklin Lake, NJ) at 1:33 were used. Some antibodies to identify cell types were also used. As antibodies to the neuronal marker, monoclonal mouse anti-NeuN antibody (1:1000; Chemicon, Temecula, CA) and polyclonal goat anti-DCX antibody (1:100; Santa Cruz Biotechnology, Santa Cruz, CA) were used. The reaction time of NeuN was 1 d and that of DCX was 3 d. As antibodies to the astroglial marker, polyclonal rabbit anti-GFAP antibody (1:10,000; Dako, Carpinteria, CA) and polyclonal rabbit anti-S-100β antibody (1:5000; Swant, Bellinzona, Switzerland) were used. As the antibody to oligodendrocyte marker, monoclonal mouse IgM anti-O4 antibody (1:10; Chemicon) was used. Then, as the antibody to microglial marker, polyclonal rabbit IgG anti-Iba-1 antibody (1:250; kind gift from S. Kohsaka, National Institute of Neuroscience, Tokyo, Japan) was used. The reaction time of GFAP, O4, and Iba-1 was 1 d and that of S-100β and O4 was 3 d. After immunoreaction with these primary antibodies, sections were washed with TBS. The sections were then reacted with fluorochromo-conjugated secondary antibodies. As secondary antibodies, Alexa 488 (1:1000; Molecular Probes, Eugene, OR) and rhodamine Red-X (1:200; Jackson ImmunoResearch, West Grove, PA) were used. Similarly as with the primary antibody, the sections were put into secondary antibodies dissolved in the blocking solution and incubated for 2 hr at room temperature with gentle shaking. The sections were then washed with TBS. The stained sections were mounted on glass slides and incubated for 15 min in DAPI (Sigma, St. Louis, MO) dissolved in 0.1% Triton X-100 in TBS and then coverslipped by using Immu-Mount (Shandon, Pittsburgh, PA) with 2% 1,4-diazabiccydo-2,2,2-octane (Sigma).

Confocal imaging and data analysis. Stained sections were observed using confocal laser scanning microscopy (TCS SP2; Leica, Wetzlar, Germany). Obtained image data were processed using image processing software (LCS; Leica) and reconstructed to three-dimensional (3D) images. With this software, a cross section of the scanning area can be confirmed, and the acquired image data can be analyzed in greater detail.

Quantification of BrdU-labeled cells. Three coronal sections of the anterior, middle, and posterior parts of the principal sulcus and central sulcus were prepared. Then, BrdU-labeled cells were counted in both banks of the principal sulcus and central sulcus by using a fluorescent microscopy (Olympus BX50, Tokyo, Japan). Furthermore, in the ventral part of area 14 (rectus gyrus) on the section of the principal sulcus, BrdU-labeled cells were also counted.

Results

As reported by previous investigators, we observed a number of BrdU-labeled cells in the cerebral cortex of each monkey (Table 1). The region of rectus gyrus (area 14) in juvenile *M. fuscata* II had the highest frequency of BrdU+ cells (88.7 cells per cubic millimeter) among all the cortical regions. The principal sulcus of the frontal association cortex had a higher frequency of BrdU-labeled cells than the motor cortex and the somatosensory cortex. BrdU-labeled cells were detected in the white matter as well as the cortex. Among the four monkeys, *M. fascicularis* I had the highest frequency of BrdU-labeled cells in the white matter. However, we did not detect any stream of BrdU-labeled cells within the white

Table 1. Number of BrdU-labeled cells in the frontal cortex of Macaque monkeys

Animal	Age (years)	BrdU injections: Number of injections	BrdU injections: Survival time[a]	Number of BrdU-labeled cells per cubic millimeter: Principal sulcus[b] Cortex	Principal sulcus[b] WM	Rectus gyrus[c] Cortex	Central sulcus[d] Cortex	Central sulcus[d] WM
M. fascicularis I	5	4	10 days	28.6	43.4	27.7	19.3	24.7
M. fascicularis II	5	5	21 days	27.2	30.5	39.2	23.3	19.6
M. fuscata I	2	5	29 days	25.1	36.4	54.7	18.1	16.9
M. fuscata II	2	5	30 days	48.5	35.2	88.7	33.9	17.5

WM, White matter.

[a]Survival time represents the period between the first BrdU injection and the perfusion.

[b,d]BrdU-labeled cells were quantified in both banks of principal sulcus and central sulcus.

[c]Rectus gyrus is the same region as the ventral part of area 14.

matter, which might indicate cell migration from the subventricular zone (SVZ) to the cerebral cortex. In the SVZ, all four monkeys had BrdU-labeled cells, but the largest number of BrdU-labeled cells appeared to be in the SVZ of *M. fascicularis* I, which had a single injection of BrdU 24 hr before it was killed (data not shown). In the cerebral cortex, some of the BrdU-labeled cells were clearly glial and endothelial cells. To determine the phenotypes of these BrdU-labeled cells, we used glial cell markers. As a result, few BrdU+ cells (<1%) were colabeled with S-100β, the astroglial marker, and then few BrdU+ cells (< 1%) expressed Iba-1, the microglial marker (Fig. 2*A–J*).

To investigate the possibility that BrdU+ cells are colabeled with the neuronal marker, sections were double-stained with BrdU and NeuN. Some BrdU-labeled nuclei appeared to be co-labeled with NeuN and, on initial inspection of our material, could be indicative of newly generated neurons (Fig. 3*A*). In such cases, we performed a detailed confocal z-series analysis, which revealed that most of these BrdU-labeled nuclei actually belonged to cells that were closely apposed to neurons but were themselves immunonegative for NeuN (Fig. 3*B–I*). This part of our findings is very similar to the results reported by Kornack and Rakic (2001a). Those flat BrdU+ cells, which are usually sticking to the cell body of neurons, are anatomically known to be satellite glial cells. In the prefrontal cortex of a young adult *M. fascicularis* II or juvenile *M. fuscata* II, 37.4 or 35.7%, respectively, of all BrdU+ cells were satellite glial cells, which were not stained with glial markers such as GFAP, S-100β, O4, and Iba-1.

To characterize and quantify the remaining population of BrdU+ cells, we performed an extensive double-staining immunohistochemical analysis of the prefrontal cortex as well as other areas of the cerebral neocortex. We found only 18 BrdU+/NeuN+ cells in the >500 cortical slices from four monkeys. Because each slice possesses between 300 and 1400 BrdU+ cells, this incidence of BrdU+/NeuN+ cells is between 18 in 150,000 and 18 in 700,000 (0.0026–0.012%). However, because each animal received four or five BrdU injections, the number labeled per day has to be considerably smaller. Nine of 18 BrdU+/NeuN+ cells were localized in the principal sulcus, and five were observed in the ventral part of area 14. However, the localization of NeuN protein was limited to the cell nucleus (Figs. 4 *A–E*, 5*A–J*), which was not the case with the surrounding neurons. Furthermore, the oval, triangular, or spindle-shaped nuclei of these cells were significantly smaller than of any cortical neurons in the same tissue. Because NeuN may not be a definitive neuronal marker (Wolf et al., 1997; Teo et al., 1999), we also performed anti-DCX staining, which labels perinuclear cytoplasm of migrating young neurons (Gleeson et al., 1999; Nacher et al., 2001). With this method, we observed two BrdU+ cells that were weakly costained with this marker in >100 slices examined (Fig. 4*F–J*). This is an incidence

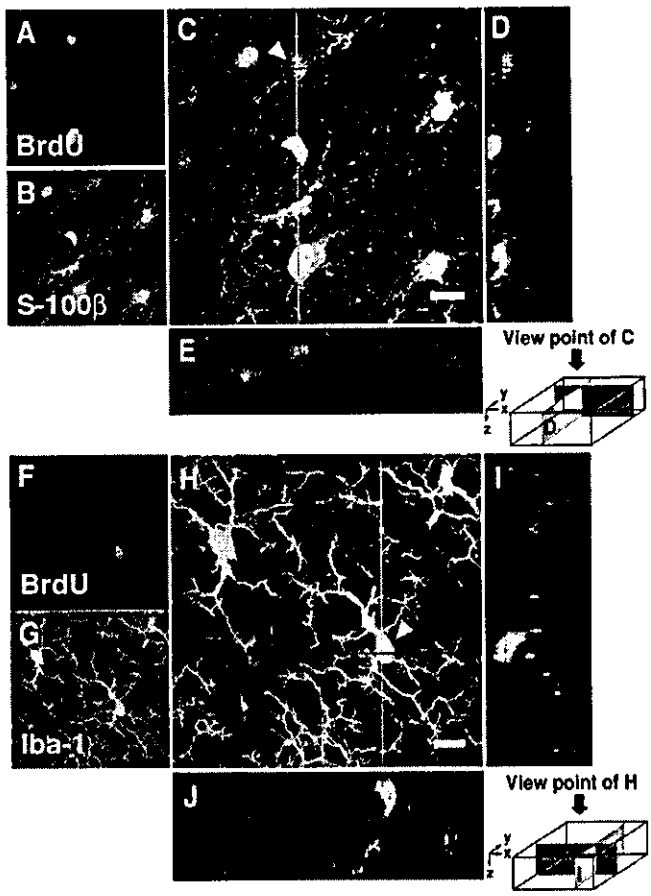

Figure 2. 3D images of BrdU+ cells double-labeled with glial markers in the prefrontal cortex of Macaque monkeys. *A–E*, A cell double-labeled with BrdU and S-100β (astroglial marker indicated by *arrowhead*). *A–C*, Images projected from a stack of 42 optical slices at a 0.5 μm interval. *A*, BrdU (*red*). *B*, S-100β (*green*). *C*, Overlay. *D*, The *y–z* cross section of the *red line* of *C*. *E*, The *x–z* cross section of the *blue line* of *C*. *F–J*, A cell double-labeled with BrdU and Iba-1 (microglial marker indicated by *arrowhead*). *F–H*, Images projected from a stack of 53 optical slices at a 0.5 μm interval. *F*, BrdU (*red*). *G*, Iba-1 (*green*). *H*, Overlay. *I*, The *y–z* cross section of the *red line* of *H*. *J*, The *x–z* cross section of the *blue line* of *H*. Scale bars, 8 μm.

of <2 in 30,000 which is a lower rate of double-positive cells than we detected with NeuN and BrdU. In addition, those BrdU+/DCX+ cells were substantially less intensely stained with DCX antibody than the migrating cells observed in the olfactory bulb of the very same animals (see below). At any rate, DCX antibody was reported to stain nondividing cells in the brain regions where there are no new neurons, such as the corpus callosum (Nacher et al., 2001), and thus those faintly stained cells cannot be taken as evidence for migrating neurons in the cortex.

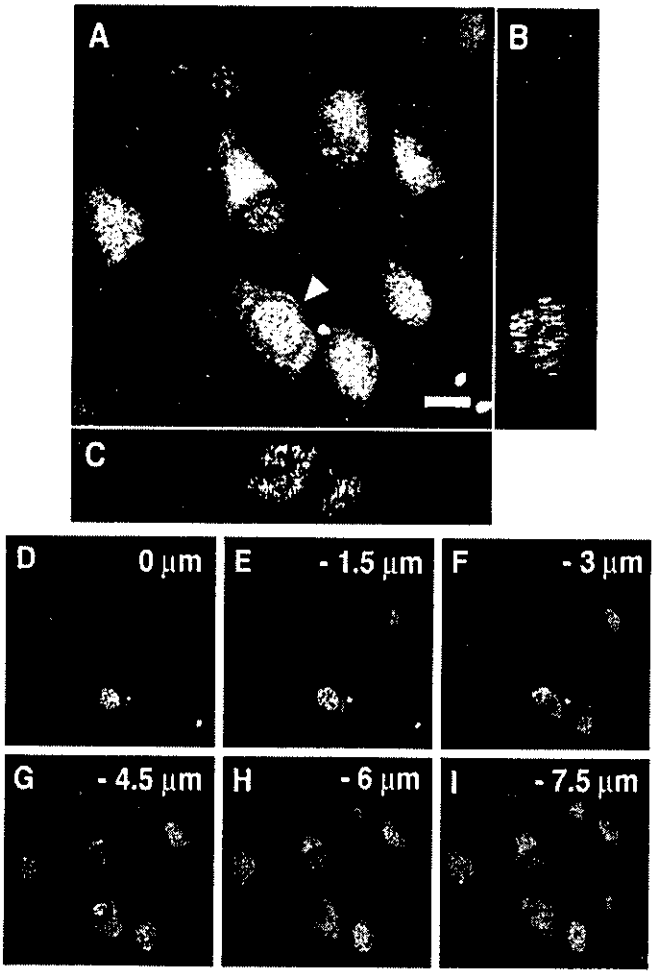

Figure 3. 3D images of a BrdU-labeled satellite glial cell. *A*, An image projected from a stack of 36 optical slices at a 0.5 μm interval. A cell double-labeled with BrdU (*red*) and NeuN (*green*) appears to be found (*arrowhead*). Scale bar, 8 μm. *B*, *C*, In fact, in the cross sections, the cell is not double-labeled. A BrdU-labeled cell is closely apposed to the soma of a NeuN-labeled neuron. *B*, The *y–z* cross section of *A*. *C*, The *x–z* cross section of *A*. *D–I*, Six different optical slices at a 1.5 μm interval of *A* also indicate that these are two separate cells.

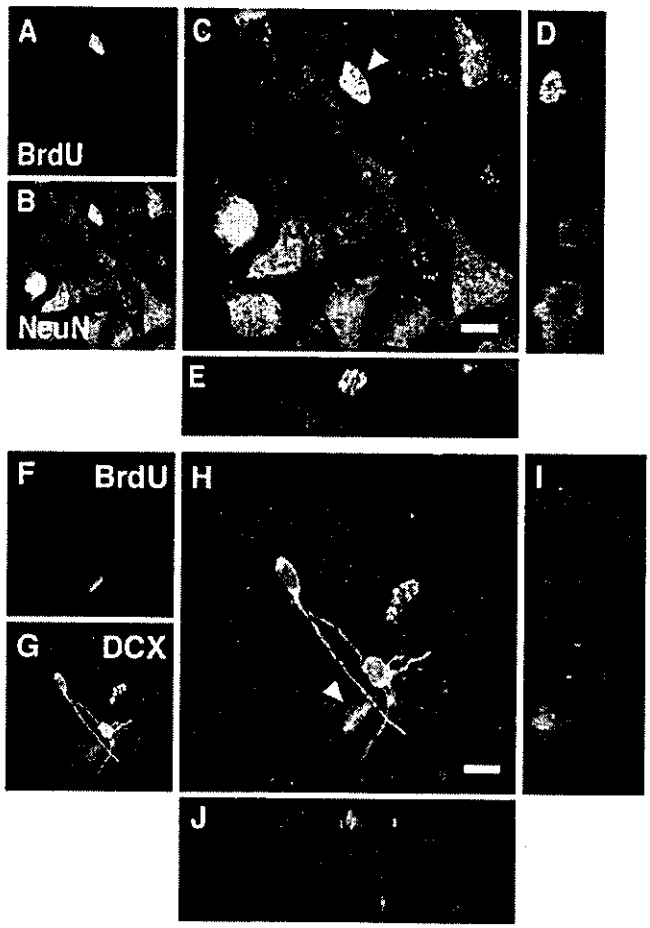

Figure 4. 3D images of BrdU+ cells in the prefrontal cortex of a juvenile Macaque monkey. *A–E*, A cell double-labeled with BrdU and NeuN (*arrowhead*). The localization of NeuN protein in the double-labeled cell is limited to the cell nucleus. *A*, BrdU (*red*). *B*, NeuN (*green*). *C*, Overlay. *D*, The *y–z* section view of *C*. *E*, The *x–z* section view of *C*. *F–J*, A cell double-labeled with BrdU and DCX (*arrowhead*). The DCX staining of the double-labeled cell is weak. *F*, BrdU (*red*). *G*, DCX (*green*). *H*, Overlay. *I*, The *y–z* section view of *H*. *J*, The *x–z* section view of *H*. Scale bars, 8 μm.

To check the validity and reliability of our methods, we examined the presence and nature of BrdU-labeled cells in the olfactory bulb where new neurons have been reported to exist in monkeys (Kornack and Rakic, 2001b) by using juvenile *M. fuscata*. Indeed, in the olfactory bulb we observed BrdU+/NeuN+ cells situated around the glomerular layer of the olfactory bulb (Fig. 6*A–E*). Judging from their size and shape, these cells seemed to be interneurons. We usually observed several BrdU+/NeuN+ cells per sagittal section of the olfactory bulb, clearly demonstrating the presence of a small but consistent number of newborn neurons in the olfactory bulb in this species. This incidence is therefore at least 100 times greater than the incidence of BrdU+/NeuN+ neurons in the prefrontal cortex. This finding stands in contrast to the lack of such cells in the cerebral neocortex of the very same specimens stained with the same method. Importantly, we observed a number of BrdU+/DCX+ double-stained cells located just away from the subventricular zone of the olfactory bulb (Fig. 6*F–J*). The DCX staining of these cells was strong and located over the cytoplasm, equivalent to the staining of the neighboring neurons. Together, our comparative analysis reveals a small but steady cell turnover of interneurons in the olfactory bulb and the absence of such turnover in the cortical areas examined in the same specimens. This indicates that the methods that we have used are suitably sensitive to detect neuron production when it is present.

Discussion

The present study was conducted in two different species of Macaque monkeys that have been maintained in an environment enriched with toys and social interactions. We applied the most advanced methods of labeling new cells and their phenotypes. Our comprehensive and detailed analysis shows that although there is an easily detectable amount of cell proliferation that leads to BrdU-labeled cells in the cerebral cortex, we could not unequivocally identify a single, newly produced neuron. Thus, our results support the concept that neuronal populations of the cerebral neocortex in healthy, sexually mature primates become stable and are normally nonrenewable (Rakic, 1985; Kornack and Rakic, 2001a). Most of the BrdU-labeled cells in the neocortex were non-neuronal, and few (<2%) of them were stained with glial markers such as S-100β and Iba-1. Satellite glial cells (35–38%), which generally are closely adhered to the surface of neocortical neurons, turned out not to be stained with any of the glial markers that we used (GFAP, S-100β, O4, and Iba-1). These satellite glial cells have been observed previously in the substantia nigra of adult rat (Lie et al., 2002). They also did not determine

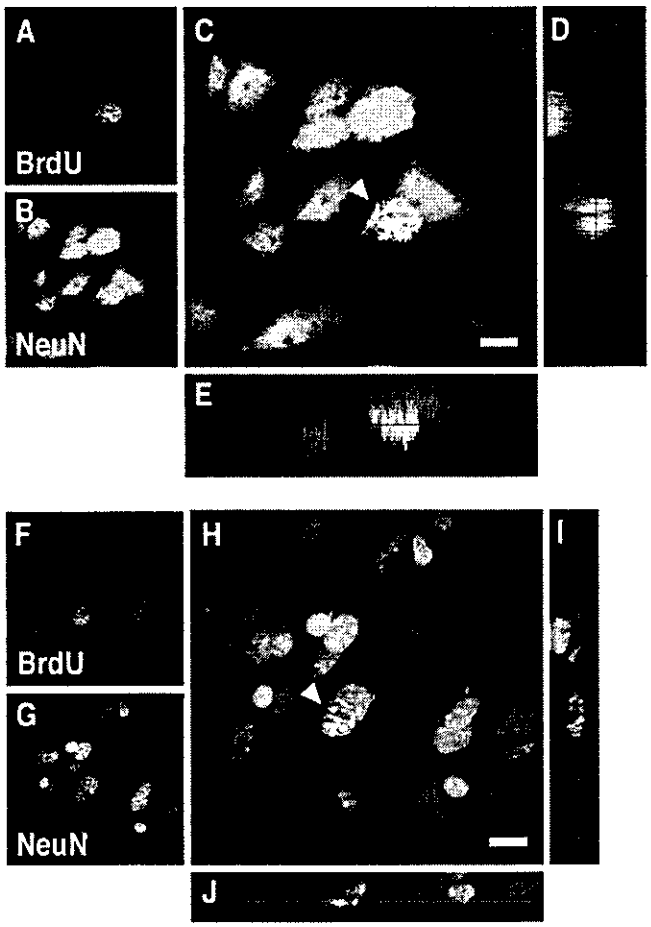

Figure 5. 3D images of cells double-labeled with BrdU and NeuN in the prefrontal cortex of a young adult Macaque monkey. *A–E*, A cell double-labeled with BrdU and NeuN (*arrowhead*) in the prefrontal cortex of *M. fascicularis* I. The localization of NeuN protein in the double-labeled cell is limited to the nucleus. *A*, BrdU (*red*). *B*, NeuN (*green*). *C*, Overlay. *D*, The *y–z* section view of *C*. *E*, The *x–z* section view of *C*. *F–J*, A cell double-labeled with BrdU and NeuN (*arrowhead*) in the prefrontal cortex of *M. fascicularis* II. As in *M. fascicularis* I, the distribution of NeuN protein is localized in the nucleus. *F*, BrdU (*red*). *G*, NeuN (*green*). *H*, Overlay. *I*, The *y–z* section view of *H*. *J*, The *x–z* section view of *H*. Scale bars, 8 μm.

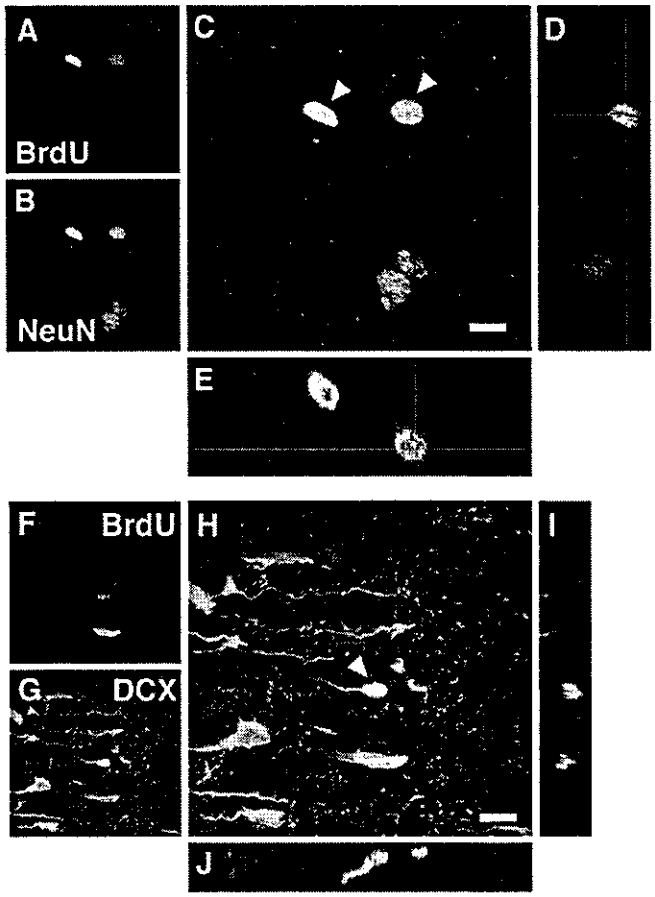

Figure 6. 3D images of BrdU+ cells in the olfactory bulb of a juvenile Macaque monkey. *A–E*, Two cells double-labeled with BrdU and NeuN (*arrowheads*) are located around the glomerular layer. *A*, BrdU (*red*). *B*, NeuN (*green*). *C*, Overlay. *D*, The *y–z* section view of *C*. *E*, The *x–z* section view of *C*. *F–J*, A cell double-labeled with BrdU and DCX (*arrowhead*) is located on the rostral migratory stream as it enters the olfactory bulb. *F*, BrdU (*red*). *G*, DCX (*green*). *H*, Overlay. *I*, The *y–z* section view of *H*. *J*, The *x–z* section view of *H*. Scale bars, 8 μm.

the phenotype of these satellite glial cells. In the end, we could not determine the phenotype of the rest (~60%) of the BrdU-labeled cells.

Of a total of several hundred thousand BrdU-labeled cells observed, only 18 NeuN and 2 DCX double-labeled cells could be found. Importantly, the size, shape, and staining properties of these cells differed from the neurons in the adjacent neocortex, and the double labeling of these cells was qualitatively different from that which we observed in the olfactory bulb. Furthermore, DCX protein can be expressed in differentiating neurons and does not necessarily indicate that the immunostained neuron is new or migrating (Nacher et al., 2001). This casts doubt on the identity of any of these cells as newly produced neurons. Thus, our extensive examination of the tissue from juvenile and young adult Macaque monkeys did not reveal evidence of the turnover of neurons in the prefrontal or any other area of the cerebral neocortex.

What cell type are the small BrdU+/NeuN+ cells that are occasionally encountered within the primate cerebral cortex? One possibility is that some of them are degenerating neurons that increase their DNA synthesis in response to damage (Sanes and Okun, 1972; Klein et al., 2002) or as a component of naturally occurring programmed cell death (Yang et al., 2001). Second, the BrdU label might come from the blood-derived stem cells fused with neurons (Steindler and Pincus, 2002; Terada et al., 2002; Wurmser and Gage, 2002). Third, some cells could be intrinsic multipotent progenitors that express this protein but are normally prevented from differentiating into mature cortical neurons in the cortical environment (Kukekov et al., 1999; Gage, 2000; Laywell et al., 2000). Finally, there is the possibility that some of them are glial progenitors that potentially give rise to NeuN+ tumors (Wolf et al., 1997; Teo et al., 1999). Importantly, even if they are neurons, the incidence would be very small (perhaps, one to two neurons per day for the large portion of the prefrontal cortex that we sampled) and is consistent with the early report that the production of new neurons in the primate brain and in particular the neocortex is extremely "limited" compared with the high rate of neuronal renewal observed in brains of fish, amphibians, and some birds (Rakic, 1985).

It should be emphasized that neocortical neurons in other mammalian species, including rodents, are also generated during a restricted developmental period (for review, see Rakic, 2002a). Except for the report on granule cells in the hippocampus (Eriksson et al., 1998), there are no signs of natural neuronal turnover in the human forebrain (Seress et al., 2001). However, it was reported recently that in the neocortex of adult rodents neurogenesis could be induced under a specific neurodegenerative con-

dition, in particular after a photolytic deletion of projection neurons with the use of the retrograde transport of a dye and laser illumination (Magavi et al., 2000). A small number of potential neuronal precursors may exist in the primate cerebral cortex, but they do not normally differentiate into cortical neurons attributable to local conditions (Kirschenbaum et al., 1994; Pincus et al., 1998; Gage, 2000; Laywell et al., 2000; Steindler and Pincus, 2002). Such cells theoretically could be induced to differentiate into neurons by way of support of the conducive neurogenetic microenvironment (Leavitt et al., 1999; Laywell et al., 2000; Song et al., 2002). Therefore, if a technique and growth factor(s) capable of inducing appropriate neuronal differentiation are developed, neuronal replacement therapies for neurodegenerative disease may become possible through manipulation of endogenous neural precursors even in areas such as the primate cerebral neocortex, where neuronal replacement does not normally occur.

References

Caviness Jr VS, Sidman RL (1973) Time of origin or corresponding cell classes in the cerebral cortex of normal and reeler mutant mice: an autoradiographic analysis. J Comp Neurol 148:141–151.

Eriksson PS, Perfilieva E, Bjork-Eriksson T, Alborn AM, Nordborg C, Peterson DA, Gage FH (1998) Neurogenesis in the adult human hippocampus. Nat Med 4:1313–1317.

Gage FH (2000) Mammalian neural stem cells. Science 287:1433–1438.

Gleeson JG, Lin PT, Flanagan LA, Walsh CA (1999) Doublecortin is a microtubule-associated protein and is expressed widely by migrating neurons. Neuron 23:257–271.

Gould E, Reeves AJ, Fallah M, Tanapat P, Gross CG, Fuchs E (1999a) Hippocampal neurogenesis in adult Old World primates. Proc Natl Acad Sci USA 96:5263–5267.

Gould E, Reeves AJ, Graziano MS, Gross CG (1999b) Neurogenesis in the neocortex of adult primates. Science 286:548–552.

Gould E, Vail N, Wagers M, Gross CG (2001) Adult-generated hippocampal and neocortical neurons in macaques have a transient existence. Proc Natl Acad Sci USA 98:10910–10917.

Hicks SP, D'Amato CJ (1968) Cell migrations to the isocortex in the rat. Anat Rec 160:619–634.

Ito D, Imai Y, Ohsawa K, Nakajima K, Fukuuchi Y, Kohsaka S (1998) Microglia-specific localization of a novel calcium binding protein, Iba1. Brain Res Mol Brain Res 57:1–9.

Jackson CA, Peduzzi JD, Hickey TL (1989) Visual cortex development in the ferret. I. Genesis and migration of visual cortical neurons. J Neurosci 9:1242–1253.

Kirschenbaum B, Nedergaard M, Preuss A, Barami K, Fraser RA, Goldman SA (1994) In vitro neuronal production and differentiation by precursor cells derived from the adult human forebrain. Cereb Cortex 4:576–589.

Klein JA, Longo-Guess CM, Rossmann MP, Seburn KL, Hurd RE, Frankel WN, Bronson RT, Ackerman SL (2002) The harlequin mouse mutation downregulates apoptosis-inducing factor. Nature 419:367–374.

Kornack DR, Rakic P (1999) Continuation of neurogenesis in the hippocampus of the adult macaque monkey. Proc Natl Acad Sci USA 96:5768–5773.

Kornack DR, Rakic P (2001a) Cell proliferation without neurogenesis in adult primate neocortex. Science 294:2127–2130.

Kornack DR, Rakic P (2001b) The generation, migration, and differentiation of olfactory neurons in the adult primate brain. Proc Natl Acad Sci USA 98:4752–4757.

Kukekov VG, Laywell ED, Suslov O, Davies K, Scheffler B, Thomas LB, O'Brien TF, Kusakabe M, Steindler DA (1999) Multipotent stem/progenitor cells with similar properties arise from two neurogenic regions of adult human brain. Exp Neurol 156:333–344.

Laywell ED, Rakic P, Kukekov VG, Holland EC, Steindler DA (2000) Identification of a multipotent astrocytic stem cell in the immature and adult mouse brain. Proc Natl Acad Sci USA 97:13883–13888.

Leavitt BR, Hernit-Grant CS, Macklis JD (1999) Mature astrocytes transform into transitional radial glia within adult mouse neocortex that supports directed migration of transplanted immature neurons. Exp Neurol 157:43–57.

Lie DC, Dziewczapolski G, Willhoite AR, Kaspar BK, Shults CW, Gage FH (2002) The adult substantia nigra contains progenitor cells with neurogenic potential. J Neurosci 22:6639–6649.

Luskin MB, Shatz CJ (1985) Neurogenesis of the cat's primary visual cortex. J Comp Neurol 242:611–631.

Magavi SS, Leavitt BR, Macklis JD (2000) Induction of neurogenesis in the neocortex of adult mice. Nature 405:951–955.

Markakis EA, Gage FH (1999) Adult-generated neurons in the dentate gyrus send axonal projections to field CA3 and are surrounded by synaptic vesicles. J Comp Neurol 406:449–460.

Mullen RJ, Buck CR, Smith AM (1992) NeuN, a neuronal specific nuclear protein in vertebrates. Development 116:201–211.

Nacher J, Crespo C, McEwen BS (2001) Doublecortin expression in the adult rat telencephalon. Eur J Neurosci 14:629–644.

Nowakowski RS, Hayes NL (2000) New neurons: extraordinary evidence or extraordinary conclusion? Science 288:771.

Nowakowski RS, Hayes NL (2001) Stem cells: the promises and pitfalls. Neuropsychopharmacology 25:799–804.

Nowakowski RS, Lewin SB, Miller MW (1989) Bromodeoxyuridine immunohistochemical determination of the lengths of the cell cycle and the DNA-synthetic phase for an anatomically defined population. J Neurocytol 18:311–318.

Pincus DW, Goodman RR, Fraser RA, Nedergaard M, Goldman SA (1998) Neural stem and progenitor cells: a strategy for gene therapy and brain repair. Neurosurgery 42:858–867.

Rakic P (1974) Neurons in rhesus monkey visual cortex: systematic relation between time of origin and eventual disposition. Science 183:425–427.

Rakic P (1985) Limits of neurogenesis in primates. Science 227:1054–1056.

Rakic P (2002a) Adult corticogenesis: an evaluation of the evidence. Nat Rev Neurosci 3:65–71.

Rakic P (2002b) Adult neurogenesis in mammals: an identity crisis. J Neurosci 22:614–618.

Rochefort C, Gheusi G, Vincent JD, Lledo PM (2002) Enriched odor exposure increases the number of newborn neurons in the adult olfactory bulb and improves odor memory. J Neurosci 22:2679–2689.

Sanes JR, Okun LM (1972) Induction of DNA synthesis in cultured neurons by ultraviolet light or methyl methane sulfonate. J Cell Biol 53:587–590.

Seress L, Abraham H, Tornoczky T, Kosztolanyi G (2001) Cell formation in the human hippocampal formation from mid-gestation to the late postnatal period. Neuroscience 105:831–843.

Song H, Stevens CF, Gage FH (2002) Astroglia induce neurogenesis from adult neural stem cells. Nature 417:39–44.

Steindler DA, Pincus DW (2002) Stem cells and neuropoiesis in the adult human brain. Lancet 359:1047–1054.

Takahashi T, Nowakowski RS, Caviness VS Jr (1996) The leaving or Q fraction of the murine cerebral proliferative epithelium: a general model of neocortical neuronogenesis. J Neurosci 16:6183–6196.

Teo JG, Gultekin SH, Bilsky M, Gutin P, Rosenblum MK (1999) A distinctive glioneuronal tumor of the adult cerebrum with neuropil-like (including "rosetted") islands: report of 4 cases. Am J Surg Pathol 23:502–510.

Terada N, Hamazaki T, Oka M, Hoki M, Mastalerz DM, Nakano Y, Meyer EM, Morel L, Petersen BE, Scott EW (2002) Bone marrow cells adopt the phenotype of other cells by spontaneous cell fusion. Nature 416:542–545.

van Praag H, Schinder AF, Christie BR, Toni N, Palmer TD, Gage FH (2002) Functional neurogenesis in the adult hippocampus. Nature 415:1030–1034.

Wolf HK, Buslei R, Blumcke I, Wiestler OD, Pietsch T (1997) Neural antigens in oligodendrogliomas and dysembryoplastic neuroepithelial tumors. Acta Neuropathol (Berl) 94:436–443.

Wurmser AE, Gage FH (2002) Stem cells: cell fusion causes confusion. Nature 416:485–487.

Yang Y, Geldmacher DS, Herrup K (2001) DNA replication precedes neuronal cell death in Alzheimer's disease. J Neurosci 21:2661–2668.